Circulation

ORIGINAL RESEARCH ARTICLE

Impaired Intracellular Calcium Buffering Contributes to the Arrhythmogenic Substrate in Atrial Myocytes From Patients With Atrial Fibrillation

Funsho E. Fakuade, PhD*; Dominik Hubricht*; Vanessa Möller*; Izzatullo Sobitov, MSc; Aiste Liutkute, MSc; Yannic Döring, MSc; Fitzwilliam Seibertz, PhD; Marcus Gerloff; Julius Ryan D. Pronto, PhD; Fereshteh Haghighi, PhD; Sören Brandenburg, MD; Khaled Alhussini, MD; Nadezda Ignatyeva, PhD; Yara Bonhoff; Stefanie Kestel; Aschraf El-Essawi, MD; Ahmad Fawad Jebran, MD; Marius Großmann, MD; Bernhard C. Danner, MD; Hassina Baraki, MD; Constanze Schmidt, MD; Samuel Sossalla, MD; Ingo Kutschka, MD; Constanze Bening, MD; Christoph Maack, MD; Wolfgang A. Linke, PhD; Jordi Heijman, PhD; Stephan E. Lehnart, MD; George Kensah, PhD; Antje Ebert, PhD; Fleur E. Mason, PhD; Niels Voigt, MD

BACKGROUND: Alterations in the buffering of intracellular Ca^{2+}, for which myofilament proteins play a key role, have been shown to promote cardiac arrhythmia. It is interesting that although studies report atrial myofibrillar degradation in patients with persistent atrial fibrillation (persAF), the intracellular Ca^{2+} buffering profile in persAF remains obscure. Therefore, we aimed to investigate the intracellular buffering of Ca^{2+} and its potential arrhythmogenic role in persAF.

METHODS: Transmembrane Ca^{2+} fluxes (patch-clamp) and intracellular Ca^{2+} signaling (fluo-3-acetoxymethyl ester) were recorded simultaneously in myocytes from right atrial biopsies of sinus rhythm (Ctrl) and patients with persAF, alongside human atrial subtype induced pluripotent stem cell–derived cardiac myocytes (iPSC-CMs). Protein levels were quantified by immunoblotting of human atrial tissue and induced pluripotent stem cell–derived cardiac myocytes. Mouse whole heart and atrial electrophysiology were measured on a Langendorff system.

RESULTS: Cytosolic Ca^{2+} buffering was decreased in atrial myocytes of patients with persAF because of a depleted amount of Ca^{2+} buffers. In agreement, protein levels of selected Ca^{2+} binding myofilament proteins, including cTnC (cardiac troponin C), a major cytosolic Ca^{2+} buffer, were significantly lower in patients with persAF. Small interfering RNA (siRNA)–mediated knockdown of cTnC (si-cTNC) in atrial iPSC-CM phenocopied the reduced cytosolic Ca^{2+} buffering observed in persAF. Si-cTnC treated atrial iPSC-CM exhibited a higher predisposition to spontaneous Ca^{2+} release events and developed action potential alternans at low stimulation frequencies. Last, indirect reduction of cytosolic Ca^{2+} buffering using blebbistatin in an ex vivo mouse whole heart model increased vulnerability to tachypacing-induced atrial arrhythmia, validating the direct mechanistic link between impaired cytosolic Ca^{2+} buffering and atrial arrhythmogenesis.

Correspondence to: Niels Voigt, MD, or Fleur E. Mason, PhD, Institute of Pharmacology and Toxicology, University Medical Center Göttingen, Robert-Koch-Straße 40, 37075 Göttingen, Germany. Email niels.voigt@med.uni-goettingen.de or fleur.mason@med.uni-goettingen.de

*F.E. Fakuade, D. Hubricht, and V. Möller contributed equally.

Supplemental Material is available at https://www.ahajournals.org/doi/suppl/10.1161/CIRCULATIONAHA.123.066577.

For Sources of Funding and Disclosures, see pages 557–558.

Circulation is available at www.ahajournals.org/journal/circ

CONCLUSIONS: Our findings suggest that loss of myofilament proteins, particularly reduced cTnC protein levels, causes diminished cytosolic Ca^{2+} buffering in persAF, thereby potentiating the occurrence of spontaneous Ca^{2+} release events and atrial fibrillation susceptibility. Strategies targeting intracellular buffering may represent a promising therapeutic lead in persAF management.

Key Words: atrial fibrillation ■ atrial remodeling ■ calcium signaling ■ cardiac arrhythmias ■ electrophysiology ■ ion channels

Editorial, see p 560

Clinical Perspective

What Is New?

- Here we provide the first in-depth analysis of cytosolic Ca^{2+} buffering in human atrial cardiac myocytes.
- We demonstrate that cytosolic Ca^{2+} buffering is reduced in persistent atrial fibrillation (persAF), which promotes the occurrence of arrhythmogenic Ca^{2+} waves and AF maintenance.
- By showing that myofibrillar degradation, particularly reduced expression of cTnC (cardiac troponin C), is a major contributor to altered Ca^{2+} buffering in persAF, we provide a novel mechanistic link between contractile dysfunction and the proarrhythmic substrate in atrial cardiac myocytes from patients with persAF.

What Are the Clinical Implications?

- Modulation of the intracellular Ca^{2+} buffering provides a novel target that could be exploited in the treatment of persAF.
- Clinically approved Ca^{2+} sensitizers such as levosimendan or omecamtiv mecarbil and nutritional supplements like taurine and β-alanine, possessing buffering modulatory properties, could be valuable additions to currently available therapeutics used in persAF management.

Nonstandard Abbreviations and Acronyms

AF	atrial fibrillation
AP	action potential
B_{max}	maximum buffering capacity
CaT	Ca^{2+} transient
cMyBP-C	cardiac myosin binding protein-C
Ctrl	sinus rhythm control
cTnC	cardiac troponin C
cTnI	cardiac troponin I
$I_{Ca,L}$	L-type Ca^{2+} current
iPSC-CM	induced pluripotent stem cell-derived cardiac myocyte
K_d	equillibrium dissociation constant
Myh6	myosin heavy chain 6
MLC2a	myosin light chain 2a (atrial isoform)
NCX	Na^{+}-Ca^{2+} exchanger
persAF	persistent atrial fibrillation
RyR2	cardiac ryanodine receptor type 2
SCaEs	spontaneous Ca^{2+} release events
SERCA	sarcoplasmic reticulum Ca^{2+}-ATPase
si-cTnC	small interfering RNA targeting cardiac troponin C
siRNA	small interfering RNA
SR	sarcoplasmic reticulum
Tm1	tropomyosin 1
Tm2	tropomyosin 2

Atrial fibrillation (AF) is the most frequent cardiac arrhythmia and is associated with increased mortality and morbidity.[1] Despite recent advances in the understanding of the molecular mechanisms underlying AF pathophysiology, treatment remains challenging, particularly because of the self-promoting remodeling induced by AF.[2]

Altered intracellular Ca^{2+} handling is a key contributor to AF-associated remodeling.[3–5] In healthy cardiac myocytes, Ca^{2+} enters the cell during systole through voltage-gated L-type Ca^{2+} channels ($I_{Ca,L}$) and induces a much larger Ca^{2+} release from the sarcoplasmic reticulum (SR) through SR Ca^{2+} release channels (ryanodine receptors, RyR2 [cardiac ryanodine receptor type 2]). The released Ca^{2+} binds to cTnC (cardiac troponin C) and induces contraction of myofilaments. During diastole, Ca^{2+} is pumped back into the SR by SERCA (SR Ca^{2+}-ATPase) and is extruded from the cell predominantly by the Na^{+}-Ca^{2+} exchanger (NCX). In AF, normal physiological Ca^{2+} cycling is disturbed, and RyR2 fails to remain closed during diastole.[6–8] This leads to spontaneous diastolic Ca^{2+} releases (spontaneous Ca^{2+} release events [SCaEs]), including sparks and waves, which are thought to play a major role in AF initiation and maintenance.[3,9]

It is important to note that only about 1% of cytoplasmic Ca^{2+} is free, whereas the remainder is bound to cytoplasmic Ca^{2+} buffers.[10] Therefore, it is not surprising that even minor changes in the Ca^{2+} binding properties of Ca^{2+} buffers may have a huge impact on the size and kinetics of free Ca^{2+} transients (CaT). In addition, altered Ca^{2+} buffering has been suggested to be involved in the propagation of arrhythmogenic Ca^{2+} waves.[11,12]

Because cTnC is one of the most important Ca^{2+} buffers,[10,13] and AF is associated with severe contractile dysfunction and degradation of myofilament proteins,[14–17] we hypothesize that Ca^{2+} buffering is reduced in atrial myocytes from patients with AF and that this could contribute to arrhythmogenesis in patients with AF.

In the present study, we quantified cytosolic Ca^{2+} buffering in atrial cardiac myocytes from right atrial samples of patients in sinus rhythm (control) and persistent AF (persAF). Using atrial subtype human induced pluripotent stem cell–derived cardiac myocytes (iPSC-CMs), we demonstrate that knockdown of cTnC leads to reduced Ca^{2+} buffering and increases incidence of SCaEs, thereby phenocopying the Ca^{2+} handling alterations observed in patients with AF.[3,4,7,8] Last, we use a new ex vivo mouse heart model to directly link reduced cytosolic Ca^{2+} buffering to increased atrial arrhythmogenesis. Taken together, we conclude that increasing cytosolic Ca^{2+} buffering may represent a novel therapeutic strategy to improve atrial contraction and reduce arrhythmogenesis in patients with AF.

METHODS

A detailed description of all methods is provided in the Supplemental Material.

Experimental protocols were approved by the ethics committees of Göttingen University (No. 10/9/15, 15/2/20 and No. 4/11/18) and conducted following the Declaration of Helsinki. Each patient gave written informed consent.

The data that support the findings of this study are available from the corresponding authors upon reasonable request.

Human Tissue Samples and Myocyte Isolation

Right atrial appendages were obtained from sinus rhythm patients (Ctrl) and patients in long-term persAF undergoing open-heart surgery (Tables S1 through S3). Excised right atrial appendages were either snap-frozen in liquid nitrogen for biochemical studies or subjected to a standard protocol[3,18] for myocyte isolation. Right atrial myocytes were suspended in EGTA-free storage solution for subsequent simultaneous measurement of cellular electrophysiology and $[Ca^{2+}]_i$ (Figure S1).

Cardiac Differentiation of Human iPSCs and Small Interfering RNA–Mediated cTnC Knockdown

Atrial iPSC-CMs were generated by subtype-directed differentiation of iPSCs from healthy donors, as previously described.[19–21] In brief, directed feeder-free cardiac differentiation of iPSC lines was achieved through canonical WNT modulation with small molecules CHIR (day 0) and IWP2, followed by metabolic selection with lactate. For atrial subtype specification, 1 µmol/L retinoic acid (Sigma Aldrich) was added between day 3 and day 6. Between day 27 and day 30, purified iPSC-CMs were digested with TrypLE (Thermo Fisher Scientific) and sparsely plated on 1:60 Matrigel-coated borosilicate glass 10-mm No. 0 round coverslips at a density of 15 000 cells/cm^2.

Human atrial iPSC-CMs in culture were transfected for 48 hours using predesigned small interfering RNAs (siRNAs) targeting the cardiac troponin C 1 gene (*TNNC1*; Thermo Fisher, s14273) or nonsilencing negative control siRNA (Thermo Fisher, 4390843) following provided manufacturer instructions. Transfected cells were used for subsequent downstream experiments.

Intracellular Calcium Measurement and Cellular Electrophysiology

Only rod-shaped myocytes with clear striations and defined margins, as observed in brightfield mode with the microscope ocular, were selected for measurements of $[Ca^{2+}]_i$ and cellular electrophysiology. $[Ca^{2+}]_i$ of right atrial myocytes was measured using the fluorescent Ca^{2+} indicator Fluo-3 AM, according to our previously published protocol.[3] Simultaneously, the whole-cell ruptured patch-clamp technique was used to record membrane currents at 37 °C.[3] Membrane currents were related to membrane capacitance and expressed in current density (pA/pF). Measurements of Ca^{2+} entry (integrated $I_{Ca,L}$) and SR Ca^{2+} content (integrated caffeine induced trainsient inward current) are expressed per liter total cell volume, which has been estimated based on a capacitance to volume relationship. Capacitance to volume relationship of atrial iPSC-CMs was estimated based on previously published data (4.57 pF/pL).[22]

Ca^{2+} sparks in Fluo-4 AM–loaded atrial iPSC-CMs were measured in separate experiments using a LSM 5 confocal microscopy system (Carl Zeiss, Jena, Germany) with a 40× oil objective in line-scan mode (512 pixels, 37.5 µm, 1302 Hz, 10 000 cycles, pinhole 67 µm) and Zen 2009 acquisition software. Field stimulation (2 Hz) was applied to myocytes for approximately 20 s, after which confocal line scans were performed during rest.

Optical action potentials (AP) were measured under field stimulation in 0.1× Fluovolt (Thermo Scientific)–loaded atrial iPSC-CMs in a bath solution containing (in mmol/L) $CaCl_2$ 2, glucose 10, HEPES 10, KCl 4, $MgCl_2$ 1, NaCl 140; pH=7.35 was adjusted with NaOH, on the heated (37 °C) stage of an epifluorescence microscope (λ_{ex}=470 nm, λ_{em}=535 nm), optimized for high-speed photomultiplier signal capture.[23,24]

Determination of Atrial Cell Volume

A modification of the approach used by Walden et al[25] was used to determine the capacitance to volume relationship in atrial myocytes, allowing Ca^{2+} fluxes and SR Ca^{2+} content to be expressed relative to total cell volume. Atrial myocytes from patients were loaded with the membrane-staining dye di-4-ANEPPS (2 µmol/L, 2 minutes) and imaged using serial z stacks (0.16 µm thickness, 63×1.2 NA water immersion objective, λ_{ex}=488 nm, and λ_{em}=500–783 nm). Cell volume was calculated by multiplying the cross-sectional area with the z interval and assuming an accessible fraction of 0.65.

Skinned Fiber Preparation and Force Measurements

Skinned fibers were prepared as described previously.[26] Resected muscle fibers were incubated for 24 hours in a 1% Triton X-100 solution for membrane permeabilization. After this skinning process, muscle strips were prepared (2–2.5 mm×0.3 mm).

For force measurements muscle fibers were installed in a force transducer system (Scientific Instruments, Heidelberg, Germany) and perfused with relaxation buffer containing (in mmol/L) imidazole 68, creatine phosphate 327, sodium azide 65, ethyleneglycol tetraacetic acid 380, $MgCl_2$ 203, dithioerythritol 154, ATP 605, and creatine kinase 400 U/mL. Free Ca^{2+} was increased stepwise according to Fabiato and Fabiato for measurement of contraction.[27]

Biochemical Studies

Expression of myofilament proteins was quantified by immunoblot, as previously described,[3,28,29] and normalized to calsequestrin, which was unchanged in persAF compared with control samples (Tables S4 and S5).

Langendorff Experiments

All animal procedures were reviewed and approved by the Institutional Animal Care and Use Committee in compliance with European Union Directive 2010/63/EU, and with the current version of the German Law on the Protection of Animals. Mouse hearts were perfused retrogradely on a Langendorff system, and 3 electrodes were placed on the epicardial surface to measure whole-heart and atrial electrophysiology. In addition, a stimulating electrode was used. To reduce the threshold for atrial arrhythmia induction, hearts were perfused with solution containing decreasing concentrations of potassium (5.4, 3.7, and 2.0 mmol/L). Diazoxide (300 μmol/L)[30] was added to the perfusing solution (2.0 mmol/L potassium) as a final step. At each potassium concentration, various electrophysiological measurements were made, including the absolute refractory period and reaction to step burst pacing (400–4500 bpm) and shorter periods of high-frequency burst pacing (6000 bpm). Inducibility and duration of arrhythmic activity were measured and quantified.

Statistical Analysis

Normally distributed data (Shapiro-Wilk normality test) were compared using the unpaired 2-tailed Student *t* test. Differences between unpaired data with unequal variances were assessed using the Welch *t* test, which is indicated in the legends of all relevant figures. Nonnormally distributed data and all data sets with $n<10$ were compared with the Mann-Whitney U test. The Kruskal-Wallis test, followed by a Dunn post hoc test, was used to assess differences between 3 or more experimental groups. The simultaneous influence of 2 independent factors was appraised by using a 2-way ANOVA, followed by the Fisher Least Significant Difference post hoc test. Kaplan-Meier curves were compared using the Gehan-Breslow-Wilcoxon test. $P<0.05$ was considered statistically significant.

RESULTS

Reduced Ca^{2+} Buffering in Atrial Cardiac Myocytes From Patients With persAF

To quantify total cytosolic Ca^{2+} concentrations and cytosolic Ca^{2+} buffering, it is necessary to express sarcolemmal Ca^{2+} fluxes relative to total cell volume. Cell volume of atrial cardiac myocytes could be quantified from z-stack images, as described above (Figure 1A). The calculated volume was found to be higher in myocytes from patients with persAF, which appears to be mainly a result of cellular elongation, whereas cell width was not different (Figure 1B). Cell capacitance was measured at the beginning of electrophysiological experiments and was found to be comparable in both groups (persAF: 120.0±14.4 pF, n/N myocytes/patients=21/13 versus control: 100.5±9.4, n/N=26/16; P=0.25). We calculated the capacitance to volume ratio based on mean values of both parameters (persAF: 12.6±1.9 pF/pL, control: 14.9±2.2 pF/pL) and further analyzed the association between them, which we found to be strongly linear (Figure S2). These ratios were then applied to all individual capacitance measurements to estimate the volume of each individual cell undergoing electrophysiological measurement.

Intracellular Ca^{2+} handling was investigated by simultaneous electrophysiological (whole-cell ruptured patch) and epifluorescence measurements (Figure 1C; Figure S3). A voltage-step protocol (0.5 Hz stimulation) was used to induce $I_{Ca,L}$, and in agreement with previous findings, both peak $I_{Ca,L}$ amplitude and $I_{Ca,L}$ integral were smaller in persAF versus Ctrl (Figure 1D). Consistent with previous findings,[3] the diastolic Ca^{2+} levels tended to be higher in persAF, whereas amplitude of the $I_{Ca,L}$-triggered CaT was found to be smaller (Figure 1E).

In subsequent experiments, SR Ca^{2+} content was quantified; myocytes were stimulated for 3 to 5 minutes using the same protocol, after which they were clamped at −80 mV, and 10 mmol/L caffeine was applied, causing complete SR Ca^{2+} release (Figure 2A). Interestingly, the amplitude of the caffeine-induced CaT ("free" Ca^{2+}) was comparable in persAF versus control (Figure 2B). However "total" Ca^{2+}, calculated from the integral of the resulting inward NCX current and normalized to cell volume, was found to be lower in persAF (Figure 2C). Not only does this finding indicate smaller SR Ca^{2+} content in persAF but, taken together with the comparable amplitude of the caffeine-induced CaT, it points towards altered Ca^{2+} buffering properties in persAF. To investigate this further, intracellular buffering was quantified by plotting total Ca^{2+} against cytosolic free Ca^{2+} during the caffeine-induced CaT, as shown in the representative traces of Figure 2D. The data were fitted with a Michaelis-Menten buffer curve:

$$\left[Ca^{2+}\right]_{total} = \frac{B_{max} \cdot \left[Ca^{2+}\right]_i}{K_d + \left[Ca^{2+}\right]_i}$$

Maximum buffering capacity (B_{max}) was found to be significantly lower in persAF versus control (Figure 2E), suggesting fewer cytosolic Ca^{2+} buffers, whereas the dissociation constant, K_d, was comparable in both groups.

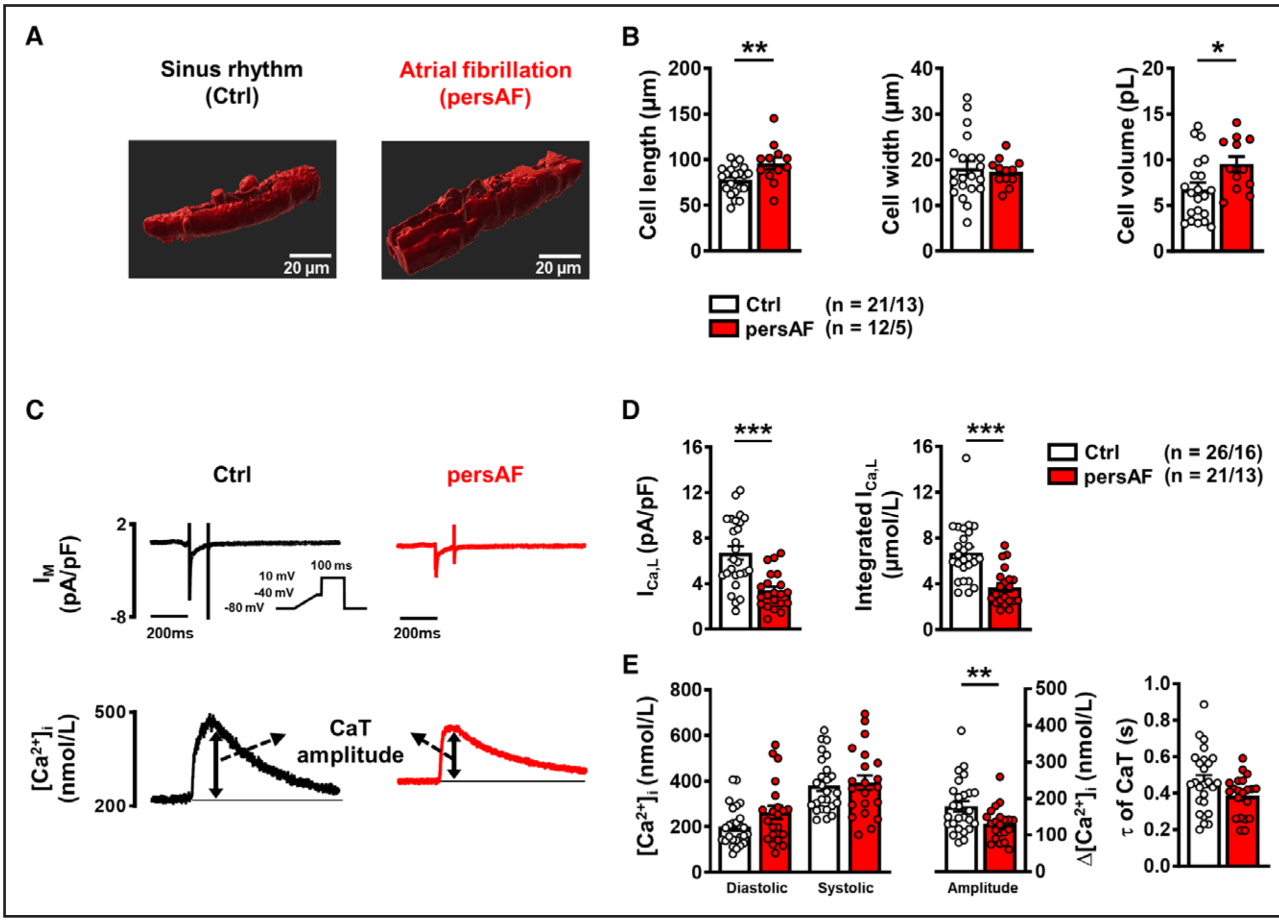

Figure 1. Characterization of atrial myocytes isolated from patients without (Ctrl) and with persAF.
A, Example 3-dimensional reconstruction of confocal z-stack images of atrial myocytes from Ctrl and persAF stained with di-4-ANEPPS. **B**, Mean±SEM cell dimensions and volume of control and persAF myocytes. **C**, $I_{Ca,L}$-triggered CaT in control and persAF atrial myocytes; representative simultaneous recordings of $I_{Ca,L}$ (**upper, inset**, voltage-clamp protocol, 0.5 Hz) and triggered CaT (Fluo-3, **lower**). **D**, Mean±SEM peak $I_{Ca,L}$ (**left**) and integrated $I_{Ca,L}$ (**right**). **E**, Mean±SEM diastolic and systolic $[Ca^{2+}]_i$ (**left**) and resulting CaT amplitude (**middle**), and time constant (τ) of decay (**right**). *$P<0.05$, **$P<0.01$, ***$P<0.001$ vs control. n/N=number of myocytes/patients. Normality of data was determined by Shapiro-Wilk test, whereas comparison was made using the Student *t* test with Welch correction and Mann-Whitney U test for normally and nonnormally distributed data, respectively. CaT indicates Ca^{2+} transient; Ctrl, control; and persAF, persistent atrial fibrillation.

Figure 2F shows total buffer power (β) (see review by Smith and Eisner[10]), which is defined as the change of total Ca^{2+} divided by that of free Ca^{2+}:

$$\beta = \frac{d\,[Ca_T]}{d\,[Ca^{2+}]} = \frac{B_{max} \cdot K_d}{([Ca^{2+}]_i + K_d)^2}$$

As previously described, total Ca^{2+} buffering represents the sum of the intrinsic Ca^{2+} buffering of the cardiac myocytes and the Ca^{2+} buffering provided by the added Fluo-3.[31] However, B_{max} remained lower in AF after correcting for the contribution of Fluo-3 to intracellular Ca^{2+} buffering (Figure S4).

Reduced Expression of cTnC Contributes to Impaired Ca^{2+} Buffering in persAF

cTnC is a major cytosolic Ca^{2+} buffer; therefore, impairment of cTnC interaction with Ca^{2+} could alter the regulation of $[Ca^{2+}]_i$ and cardiac contraction. The expression and phosphorylation of key myofilament proteins, which influence cytosolic Ca^{2+}-myofilament interaction, were determined (Figure 3A; Figure S5; Figure S6). It is interesting that expression of the cardiac troponins cTnC and cTnI (cardiac troponin I) was lower in persAF, whereas phosphorylation of cTnI was comparable between groups. Because the cardiac troponins, particularly cTnC, mediate Ca^{2+}-binding to myofilaments, lower troponin expression likely contributes to the smaller B_{max} observed in persAF. The expression of cMyBP-C (cardiac myosin binding protein-C) was also lower in persAF versus Ctrl, with preserved phosphorylation levels (Figure 3A), which, together with reduced expression of cardiac troponins, points to a loss of myofilament proteins. Furthermore, expression of Myh6 (myosin heavy chain 6) and Tm1 (tropomyosin 1) were lower in persAF, whereas expression of Tm2 (tropomyosin 2) and α-actin were comparable with Ctrl (Figure S5). Skinned muscle fibers from persAF exhibited lower maximum force than control (Figure 3B),

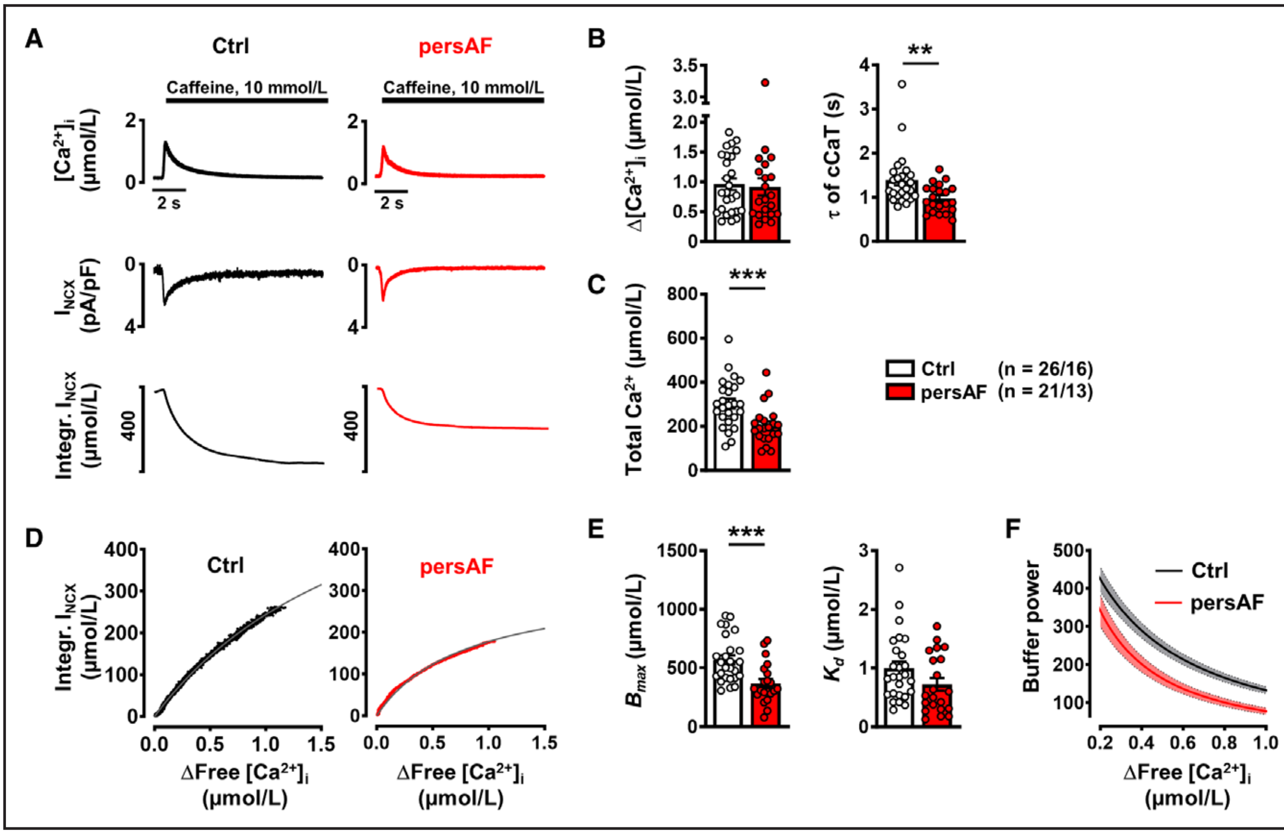

Figure 2. Caffeine-induced CaT and corresponding transient inward current (I_{NCX}) to assess SR Ca^{2+} content and buffering properties of atrial myocytes isolated from patients without (control) and with persAF.
A, Representative caffeine-induced CaT (**upper**), associated I_{NCX} (**middle**) and integral of inward current, corrected for cell volume to give a measure of total Ca^{2+} (**lower**). **B**, Mean±SEM amplitude and time constant (τ) of decay of caffeine-induced CaT. **C**, Mean±SEM calculated total Ca^{2+}. **D**, Representative buffer curves showing the relationship between cytosolic free Ca^{2+} and total Ca^{2+}, fitted with a hyperbolic function. **E**, Mean±SEM maximum buffering capacity (B_{max}, **left**) and dissociation constant (K_d, **right**), determined from buffer curves. **F**, Mean (line) ±SEM (shaded) of calculated individual total buffer power curves as a function of free $[Ca^{2+}]_i$. $^{**}P<0.01$, $^{***}P<0.001$ vs control. n/N=number of myocytes/patients. Normality of data was determined by Shapiro-Wilk test and comparison was made using the Mann Whitney U test. Ctrl indicates control; and persAF, persistent atrial fibrillation.

which may contribute to impaired fractional shortening of isolated cardiac myocytes from patients with persAF (Figure S3). Ca^{2+} sensitivity of force generation (pCa_{50}) was higher in atrial muscle fibers from patients with persAF and may represent a compensatory mechanism for the reduced maximum force in persAF. Phosphorylation of MLC2a (atrial isoform of myosin light chain) and desmin was increased in persAF (Figure S6) and may contribute to increased myofilament Ca^{2+} sensitivity.[17]

In addition to cTnC, SERCA is also an important buffer of cytosolic Ca^{2+} in cardiac myocytes.[10] To quantify SERCA activity independent of cytosolic Ca^{2+} buffering, the difference in the decay of both the total caffeine-induced CaT and total systolic CaT (calculated from buffering properties) was analyzed, as previously described.[23,32] Figure 4A shows example plots of the rate of decay of total Ca^{2+} against free Ca^{2+} concentration during the systolic CaT. The mean slope of this relationship was comparable in control and persAF. Decay of caffeine-induced CaT is SERCA-independent and results from sarcolemmal Ca^{2+} extrusion, mainly through NCX (Figure 2A). When plotting rate of decay of total Ca^{2+} against free Ca^{2+} concentration during the caffeine-induced CaT, the slope was higher in persAF, indicating faster removal of Ca^{2+} by NCX in persAF (Figure 4B). Contribution by SERCA could be ascertained by calculating the difference of the slope gradients in Figure 4A and 4B. It could be shown that SERCA contribution was comparable in control (60.7%±3.1%) and persAF (55.1%±2.6%; Figure 4C), indicating that altered buffering capacity in persAF is unlikely a result of changes in SERCA. This leaves the reduction in cTnC expression as an explanation for the reduced Ca^{2+} buffering capacity.

siRNA-Mediated cTnC Knockdown in Atrial iPSC-CM Phenocopies Ca^{2+} Buffering Characteristics of persAF

To further explore whether reduced cTnC is responsible for the altered buffering observed in persAF, an atrial iPSC-CM model with reduced cTnC protein

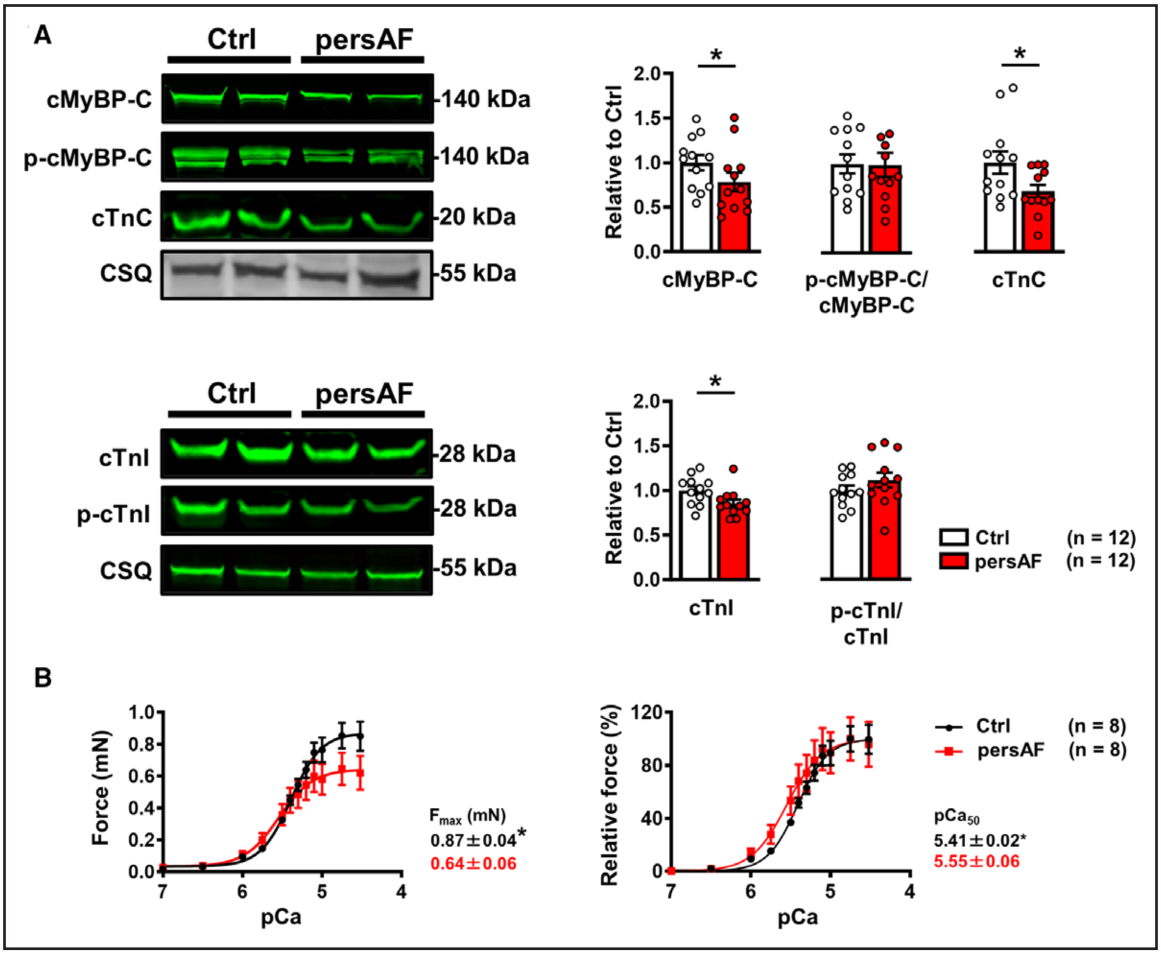

Figure 3. Myofilament protein expression and contractile response to cytosolic Ca^{2+} in control and persAF.
A, Immunoblots (**upper left**) and quantification (**upper right**) of cMyBP-C (cardiac myosin binding protein-C), its phosphorylated state (P-cMyBP-C), and cTnC (cardiac troponin-C) in atrial samples from controls and patients with persAF, normalized to CSQ (calsequestrin), except for P-cMyBP-C, which was normalized to total cMyBP-C. Immunoblots (**lower left**) and quantification (**lower right**) of cTnI (cardiac troponin I) and its phosphorylated state (P-cTnI) in atrial samples from controls and patients with persAF, normalized to CSQ and total cTnI, respectively. **B**, Absolute (**left**) and normalized (**right**) force-pCa relationship of skinned muscle fibers of controls and patients with persAF with mean±SEM of maximum force (F_{max}) and calcium sensitivity (pCa_{50}). *P<0.05 vs control. n=number of patients. Normality of data was determined by Shapiro-Wilk test, whereas comparison was made using the Student *t* test with Welch correction. Ctrl indicates control; and persAF, persistent atrial fibrillation.

expression was used. Atrial iPSC-CMs were differentiated as previously described and confirmed for atrial-specific markers (MLC2a and $I_{K,ACh}$ [acetylcholine activated inward rectifier K^+ current]; Figure S7).[19–21] cTnC knockdown was mediated by siRNA targeting cTnC (si-cTnC), and for the control group, atrial iPSC-CMs were treated with nonsilencing siRNA (Figure S8). For simultaneous epifluorescence and electrophysiological measurement, atrial iPSC-CMs were loaded with Fluo-3 AM and stimulated by voltage-clamp control in the whole cell ruptured patch configuration (Figure 5A). $I_{Ca,L}$ was induced by a voltage-step protocol (0.5 Hz stimulation), and peak current and current integral were found to be comparable in control and si-cTnC (Figure 5B), whereas the amplitude of the $I_{Ca,L}$-triggered CaT was larger in si-cTnC versus control (Figure 5C). iPSC-CMs were subsequently clamped at −80 mV, and 10 mmol/L caffeine was applied, causing total release of SR Ca^{2+} (Figure 5D). The amplitude of the caffeine-induced CaT was larger in si-cTnC; however, when the integral of the resulting inward NCX current was quantified and total Ca^{2+} was calculated, these parameters were found to be similar in si-cTnC and control, pointing to comparable SR Ca^{2+} load (Figure 5D through 5F). Intracellular buffering was quantified, as described previously, by plotting total Ca^{2+} against cytosolic free Ca^{2+} during the caffeine-induced CaT and fitting the data with a hyperbolic curve (Figure 5G). Analysis revealed that B_{max} was smaller in si-cTnC versus control, whereas K_d was comparable between both groups (Figure 5H; Figure S9), thus mimicking the Ca^{2+} buffering characteristics of persAF. In addition, buffer power was lower in si-cTnC compared with control (Figure 5I). Contribution of NCX and SERCA to cytosolic Ca^{2+} removal remained unaltered in si-cTnC iPSC-CMs (Figure S10).

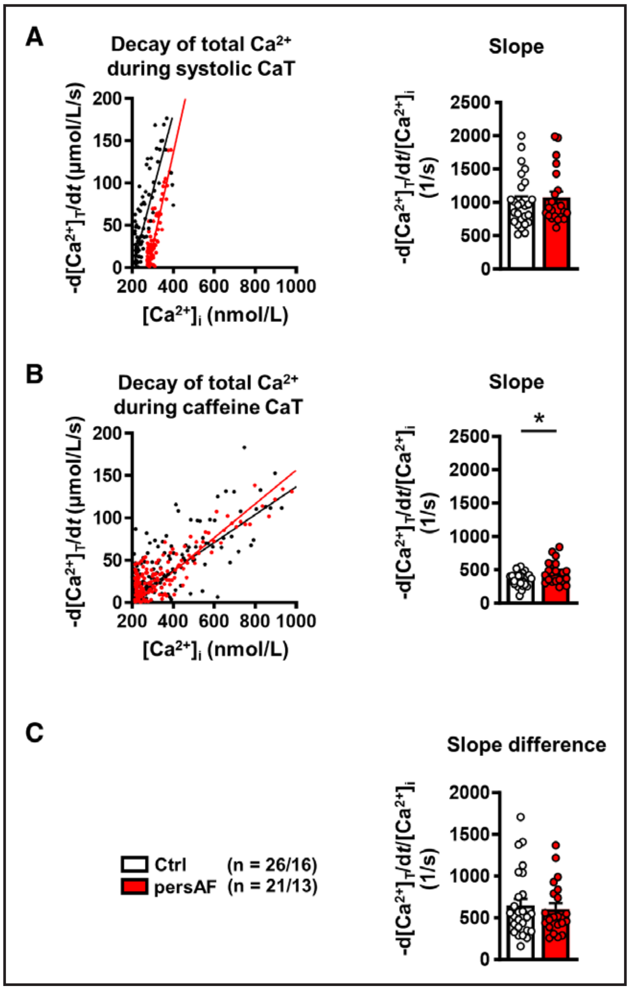

Figure 4. Quantification of decay of total Ca^{2+} in atrial myocytes isolated from patients without (control) and with persAF.

A, Representative rate of decay of total Ca^{2+} ($-d[Ca^{2+}]_T/dt$) plotted during systolic CaT against free $[Ca^{2+}]_i$ (**left**) and slope of $-d[Ca^{2+}]_T/dt$ plotted against $[Ca^{2+}]_i$ (**right**). **B**, Representative rate of decay of total Ca^{2+} during caffeine-induced Ca^{2+} transient ($-d[Ca^{2+}]_T/dt$) plotted against the corresponding free $[Ca^{2+}]_i$ (**left**) and slope of $-d[Ca^{2+}]_T/dt$ during caffeine plotted against corresponding $[Ca^{2+}]_i$ (**right**). **C**, Difference between slopes in **A** and **B**, indicating unaltered $[Ca^{2+}]_i$ dependence of SERCA-mediated Ca^{2+} removal. $^*P<0.05$ vs control. n/N=number of myocytes/patients. Normality of data was determined by Shapiro-Wilk test, whereas comparison was made using the Student *t* test with Welch correction and Mann-Whitney U test for normally and nonnormally distributed data, respectively. Ctrl indicates control; and persAF, persistent atrial fibrillation.

Potential Proarrhythmic Consequences of Reduced cTnC Levels

It has previously been shown that increased Ca^{2+} leak from the SR provides a basis for arrhythmogenesis in persAF.[3,7,8] To investigate whether reduced cytosolic Ca^{2+} buffering, specifically in the form of reduced cTnC expression, could play a proarrhythmic role, diastolic SR Ca^{2+} release was measured and quantified in atrial si-cTnC versus control (siRNA nonsilencing) iPSC-CMs. To this end, confocal line scans were performed on atrial iPSC-CMs during rest, after a brief period (20 s) of field stimulation (2 Hz). Line scan analysis revealed significantly higher Ca^{2+} spark frequency in si-cTnC compared with control (Figure 6A and 6B), indicating increased SR Ca^{2+} leak. In addition, we found increased SR Ca^{2+} leak using the previously described tetracaine protocol[33] (Figure S11). Moreover, the leak-load relationship was shifted leftward in persAF, indicating increased SR Ca^{2+} leak at any given SR Ca^{2+} content. Immunoblot analysis revealed comparable expression levels of RyR2, CaMKII, and junctophilin-2, as well as phosphorylated RyR2 and CaMKII, in si-cTnC compared with control iPSC-CMs (Figure S12).

In accordance with our in vitro experiments, computational modeling revealed that reduction of cytosolic Ca^{2+} buffering increases incidence of Ca^{2+} waves and delayed after depolarizations (Figure S13).[4,34,35]

Optical AP measurements revealed no difference in AP duration or restitution between control and si-cTnC iPSC-CMs (Figure 6C and 6D). However, the incidence of AP alternans at lower pacing frequencies was significantly larger in cells with reduced cTnC (Figure 6E and 6F). The maximum slope of the restitution curve did not exceed 1 in either group, indicating that voltage alternans of the AP is driven by intracellular Ca^{2+} aberrations.

Taken together, these data demonstrate that cTnC reduction is sufficient to reproduce the phenotype of impaired Ca^{2+} buffering observed in persAF, including increased SR Ca^{2+} leak and alternans, both of which are strongly arrhythmogenic.[3,7,8]

To ascertain whether improving Ca^{2+} buffering can ameliorate increased SR Ca^{2+} leak in si-cTnC iPSC-CMs, si-cTnC iPSC-CMs were pretreated with the Ca^{2+} sensitizer EMD57033 (5 µmol/L, pretreatment for 5 minutes),[23] and confocal line scan analysis was repeated. Although the amplitude of Ca^{2+} sparks was similar between treated and nontreated groups, Ca^{2+} spark frequency in si-cTnC iPSC-CMs was significantly reduced by EMD57033 (Figure 7A and 7B). Furthermore, Ca^{2+} spark frequency in the EMD57033-treated group was similar to that in control iPSC-CMs, thus confirming that increasing buffering can normalize SR Ca^{2+} leak.

Desensitization of Myofilaments to Ca^{2+} Causes Atrial Arrhythmia

To determine whether reduced cytosolic Ca^{2+} buffering by myofilaments alone can induce arrhythmic activity in the atria, blebbistatin was applied to Langendorff-perfused mouse hearts to reduce myofilament Ca^{2+} sensitivity, during which atrial electrograms were recorded (Figure S14). Blebbistatin significantly increased the inducibility of atrial arrhythmic activity after burst-pacing (potassium in perfusing solution: 2 mmol/L, both with and without diazoxide, Figure 8A and 8B). However, the duration of atrial arrhythmic episodes was comparable

ORIGINAL RESEARCH ARTICLE

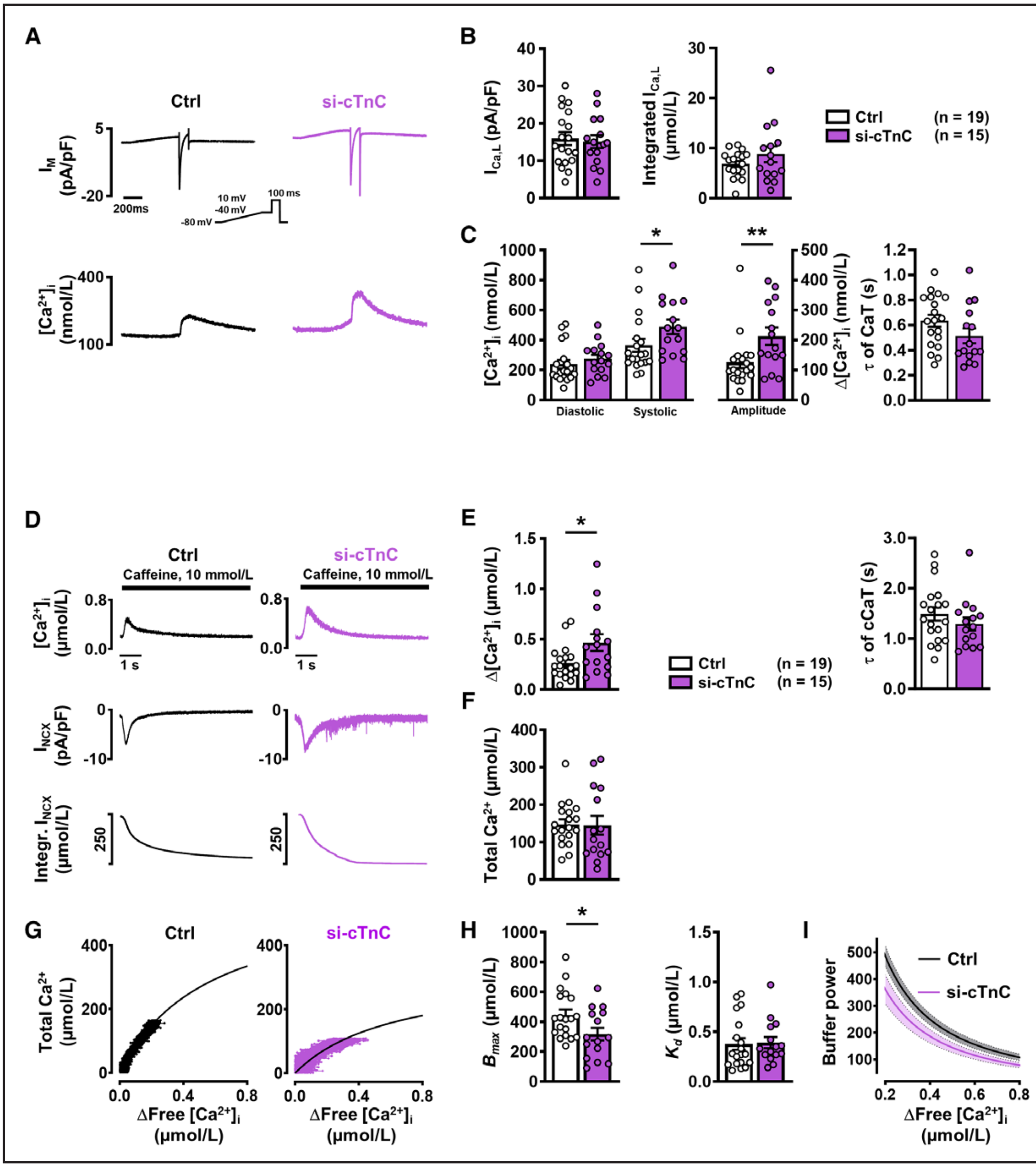

Figure 5. Ca^{2+} handling and Ca^{2+} buffering properties in atrial iPSC-CMs with normal (control) and reduced (si-cTnC) cTnC levels.

A, Representative simultaneous recordings of $I_{Ca,L}$ (**upper, inset**, voltage-clamp protocol, 1 Hz) and triggered CaT (**lower**). **B**, Mean±SEM peak $I_{Ca,L}$ (**left**) and integrated $I_{Ca,L}$ (**right**) in control (siRNA ns) and si-cTnC (siRNA cTnC) iPSC-CMs. **C**, Mean±SEM diastolic and systolic $[Ca^{2+}]_i$ (**left**) and resulting CaT amplitude (**middle**), and time constant (τ) of decay (**right**). **D**, Representative caffeine-induced CaT (**upper**), associated I_{NCX} (**middle**) and integral of inward current, corrected for cell volume to give a measure of total Ca^{2+} (**lower**). **E**, Mean±SEM amplitude (**left**) and time constant (τ) of decay (**right**) of caffeine-induced CaT. **F**, Mean±SEM calculated total Ca^{2+}. **G**, Buffer curves showing the relationship between cytosolic free Ca^{2+} and total Ca^{2+}, fitted with a hyperbolic function. **H**, Mean±SEM maximum buffering capacity (B_{max}, **left**) and dissociation constant (K_d, **right**), determined from buffer curves. **I**, Mean±SEM of calculated individual total buffer power curves as a function of free $[Ca^{2+}]_i$. *$P<0.05$, **$P<0.01$ vs control. n=number of myocytes (2–4 differentiations). Normality of data was determined by Shapiro-Wilk test, whereas comparison was made using the Student *t* test and Mann-Whitney U test for normally and nonnormally distributed data, respectively. Ctrl indicates control; cTnC, cardiac troponin C; CaT, Ca^{2+} transient; iPSC-CM, induced pluripotent stem cell–derived cardiac myocyte; ns, nonsilencing; and siRNA, small interfering RNA.

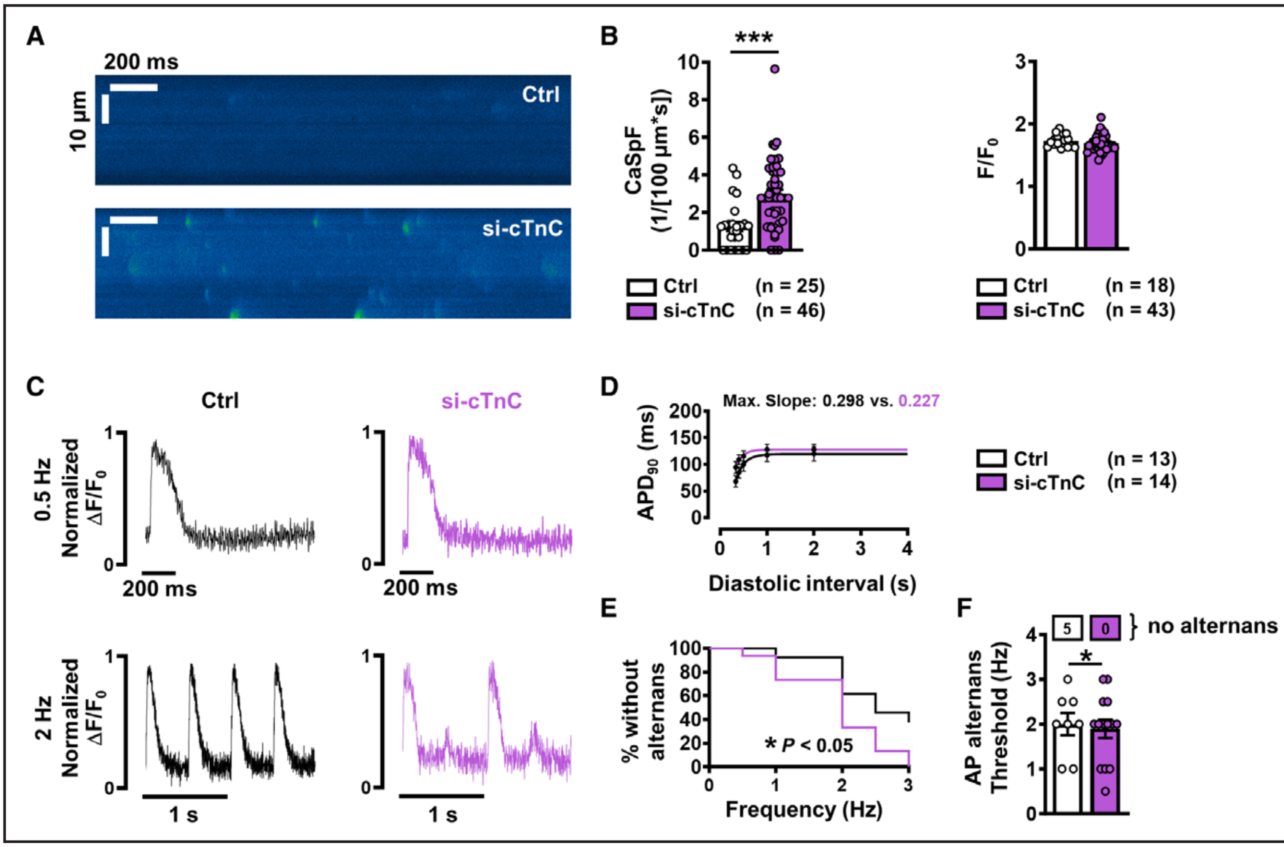

Figure 6. Incidence of Ca^{2+} sparks and action potential (AP) alternans in atrial iPSC-CMs with normal (control) and reduced (si-cTnC) cTnC levels.

A, Representative confocal line scans showing SR Ca^{2+} release in the form of Ca^{2+} sparks in control (siRNA ns) and si-cTnC (siRNA cTnC) iPSC-CMs. **B**, Mean±SEM Ca^{2+} spark frequency (CaSpF, **left**) and amplitude (**right**). **C**, Representative normalized traces of AP at 0.5 Hz (**upper**) and 2 Hz (**lower**) in control (**left**) and si-cTnC iPSC-CMs. **D**, AP duration at 90% repolarization (APD_{90}) at increasing diastolic intervals (AP restitution), fitted with a 1-phase association nonlinear function to determine maximum curve slope. **E**, Kaplan-Meier plot indicating the percentage of iPSC-CMs without alternans in relation to the respective pacing frequency. **F**, Mean±SEM alternans threshold frequency. Number of myocytes without AP alternans are shown in boxes above. $^{***}P<0.001$, $^{*}P<0.05$ vs control. n=number of myocytes (2 or 3 differentiations). Comparison was made using the unpaired Student *t* test, the Mann-Whitney U test, and the Gehan-Breslow-Wilcoxon test (**E**). Ctrl indicates control; cTnC, cardiac troponin C; iPSC-CM, induced pluripotent stem cell–derived cardiac myocyte; ns, nonsilencing; and siRNA, small interfering RNA.

even in the presence of blebbistatin (Figure 8C). Figure 8D shows a Kaplan-Meier curve of the percentage of hearts without atrial arrhythmic activity after burst pacing plotted against decreasing potassium concentrations. Blebbistatin significantly altered this curve, pointing to a higher susceptibility to atrial arrhythmic activity.

DISCUSSION

In the present study, we observed impaired cytosolic Ca^{2+} buffering in atrial myocytes from patients with persAF and analyzed the underlying molecular substrate and its contribution to atrial arrhythmogenesis. Analysis of transmembrane Ca^{2+} fluxes during systolic and caffeine-induced CaT enabled estimation of total Ca^{2+} in relation to free cytosolic Ca^{2+}. Our experiments revealed reduced total Ca^{2+} buffering capacity in persAF, likely because of degradation of myofilament proteins, which represent a major Ca^{2+} buffer in cardiac myocytes. Myofilaments play an important role in cytosolic Ca^{2+} handling, and therefore, altered myofilament expression may have direct consequences on cytosolic Ca^{2+} homeostasis. Here we demonstrate, for the first time, that reduction of cTnC expression decreases intracellular Ca^{2+} buffering and increases the incidence of both SCaEs and AP alternans in atrial iPSC-CMs, thereby phenocopying the arrhythmogenic Ca^{2+} handling phenotype observed in atrial myocytes from patients with persAF.[3,7,8]

Reduced Ca^{2+} buffering leads to a higher change in free cytosolic Ca^{2+} per total Ca^{2+} released from the SR and therefore amplifies consequences of higher incidence of SCaEs as a mechanism of increased ectopic activity in persAF. Last, reducing cytosolic Ca^{2+} buffering in an in vitro mouse model increased susceptibility to pacing-induced atrial arrhythmia, validating the direct mechanistic link between impaired cytosolic Ca^{2+} buffering and atrial arrhythmogenesis in clinical persAF.

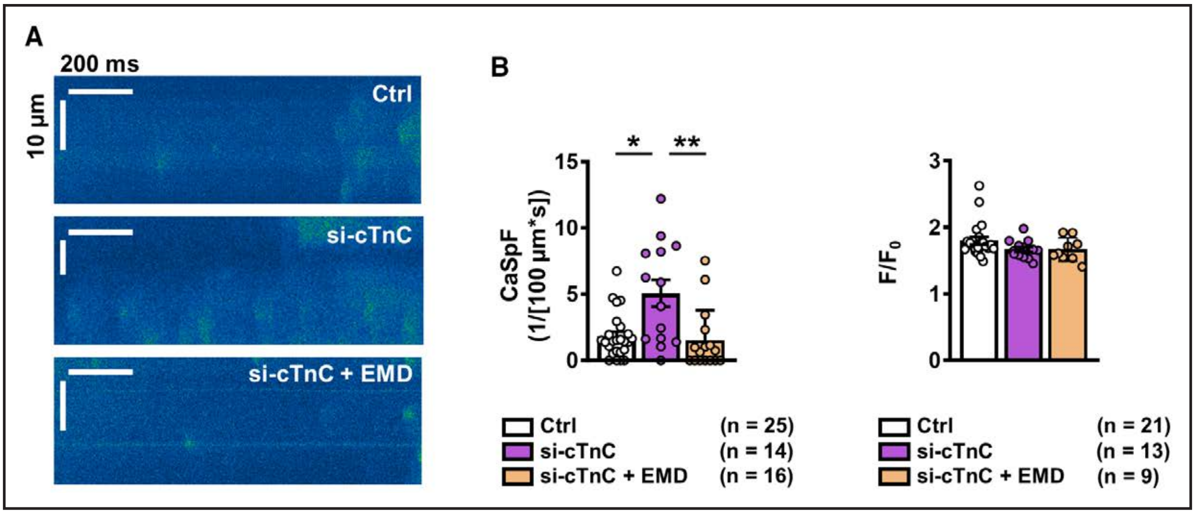

Figure 7. Effect of Ca^{2+} sensitization on Ca^{2+} sparks in atrial iPSC-CMs with reduced (si-cTnC) cTnC levels.
A, Representative confocal line scans of atrial iPSC-CMs with normal (control, siRNA ns) and reduced (si-cTnC, siRNA cTnC) cTnC levels, pretreated with EMD57033 (EMD, 5 µmol/L). **B**, Mean±SEM Ca^{2+} spark frequency (CaSpF, **left**) and amplitude (**right**). *$P<0.05$, **$P<0.01$ vs control and si-cTnC. n=number of myocytes (2 differentiations). Comparison was made using the Kruskal-Wallis test followed by the Dunn post hoc test. Ctrl indicates control; cTnC, cardiac troponin C; iPSC-CM, induced pluripotent stem cell–derived cardiac myocyte; ns, nonsilencing; and siRNA, small interfering RNA.

Impaired Contractile Function in persAF

It has been established that persAF is associated with Ca^{2+} handling abnormalities that contribute to impaired contractility and arrhythmogenesis; reduced $I_{Ca,L}$ has been widely shown to be a characteristic hallmark of AF-associated remodeling and a major contributor to AP shortening in persAF, promoting maintenance of re-entry.[3,36–38] In addition, reduced $I_{Ca,L}$ triggers smaller Ca^{2+} release from the SR, thereby contributing to impaired contractile function of atrial myocytes from persAF.

Impaired contractility is a major hallmark of AF-associated remodeling.[15,39,40] During an AF episode, contractile function of the atria is mainly constrained because of the fast and uncoordinated atrial excitation. However, the impaired contractile function persists for several weeks even after the cardioversion of AF back to sinus rhythm, leading to a high risk of atrial thromboembolism and stroke, despite sinus rhythm maintenance.[41] Similarly, force of contraction is clearly reduced in atrial preparations from patients with AF when stimulated in vitro with a constant frequency.[40] Impaired Ca^{2+} handling[40,42] and structural remodeling, including increased fibrosis, have been suggested to contribute to AF-associated contractile dysfunction.[2] Other studies of AF have shown that reduced contractility even persists in myofibril preparations lacking sarcolemma and Ca^{2+} handling machinery,[16,17] demonstrating that reduction in myofibrillar maximal active tension in persAF must be attributable to defects in the myofilaments themselves. Furthermore, and in accordance with our results, it has been shown that loss of myofilament proteins is a major mechanism contributing to impaired atrial contractility.[14,15,17,39,40,43,44] Meanwhile, mechanistic studies have revealed that degradation of cardiac troponins mainly results from increased activation of the Ca^{2+}-dependent protease calpain during high atrial stimulation frequencies,[14,43,45] suggesting that calpain inhibition may represent a future therapeutic target in preventing AF-associated contractile remodeling.

In contrast with impaired maximal force development associated with AF, our present investigation, in accordance with a previous study,[17] demonstrated higher myofilament Ca^{2+} sensitivity in atrial preparations from patients with persAF. Increased phosphorylation of MLC2a is likely a major contributor to the increased Ca^{2+} sensitivity.[46,47] However, results on phosphorylation of MyBP-C (thought to increase myofilament Ca^{2+} sensitivity) are controversial, showing increased,[17] decreased,[48] or unaltered (present study) phosphorylation levels.

Determinants of Increased Incidence of SCaEs in persAF

Increased incidence of SCaEs originating from the SR during diastole is a well-accepted mechanism underlying enhanced ectopic activity, triggering AF episodes and contributing to AF progression and maintenance.[3,5,8,9] Ca^{2+} removal from the cytosol by NCX brings 3 Na^+ ions into the cell per extruded Ca^{2+} ion. This is an electrogenic process, leading to membrane depolarizations (delayed afterdepolarizations) which, if large enough, could trigger a new AP, resulting in ectopic activity. Several mechanisms have been identified to amplify consequences of leaky RyR2 channels: (1) higher SR Ca^{2+} load, for example as a result of increased excitation frequencies in AF, escalates

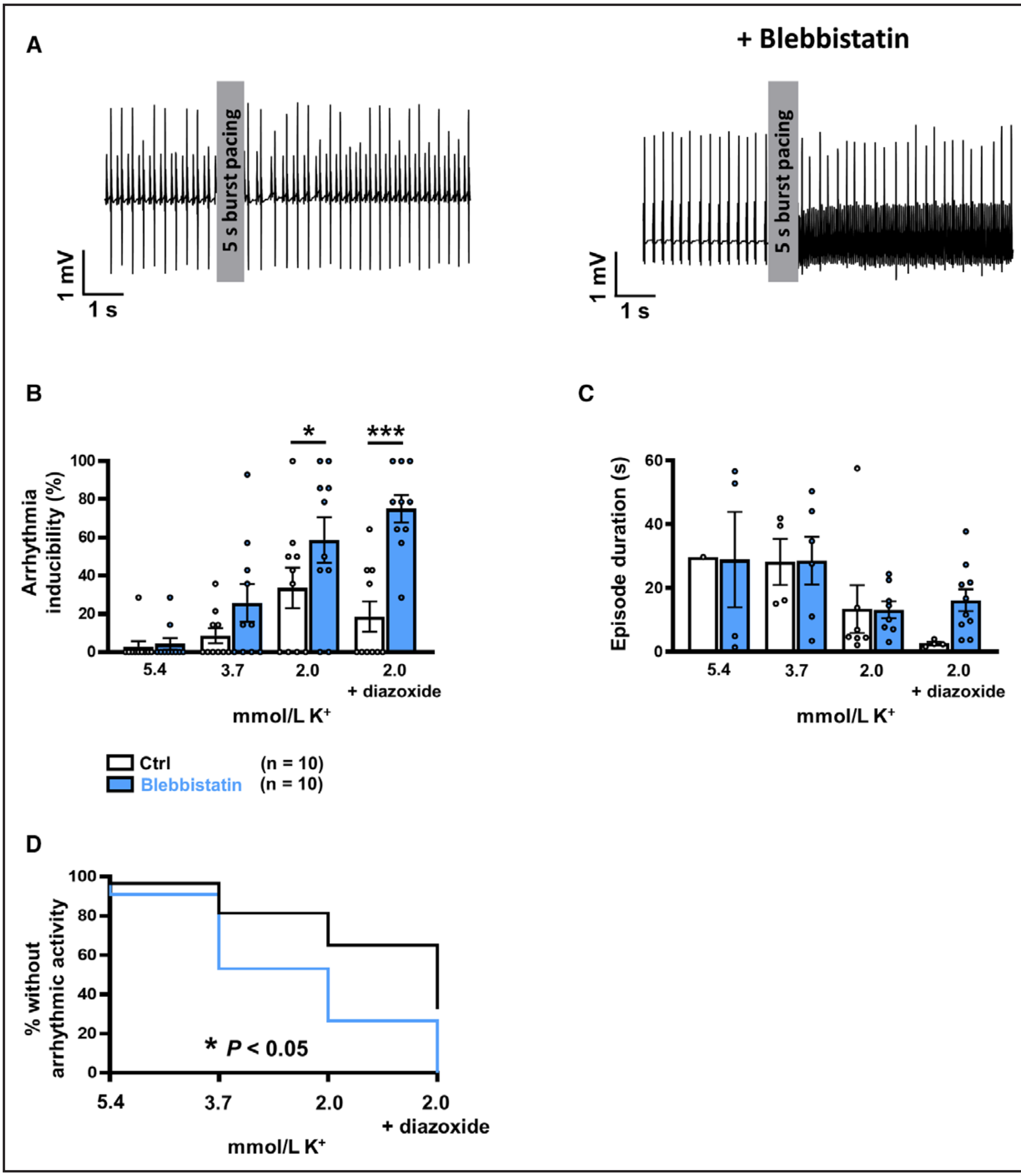

Figure 8. Langendorff experiments in mouse heart.
A, Representative atrial electrogram traces showing effect of burst pacing (100 Hz) in the absence (control, **left**) and presence (**right**) of blebbistatin (5 µmol/L) (2 mmol/L K^+ in both). **B**, Grouped bar chart showing mean±SEM inducibility of atrial arrhythmic activity for each potassium level, differentiated by the presence or absence of blebbistatin. The chart highlights significant main effects of blebbistatin, $F(1, 72)=20.06$, $P<0.0001$, and potassium, $F(3, 72)=14.91$, $P<0.0001$. **C**, Mean±SEM arrhythmic episode duration for each potassium level, in the presence or absence of blebbistatin. The graph highlights the significant effect of potassium, $F(3, 36)=3.52$, $P<0.05$. **D**, Kaplan-Meier plot showing the percentage of hearts without arrhythmic activity. $^{*}P<0.05$, $^{***}P<0.001$ vs control. n=number of hearts. Comparison using 2-way ANOVA followed by a Fisher Least Significant Difference post hoc test (**B** and **C**) and the Gehan-Breslow-Wilcoxon test (**D**). Ctrl indicates control.

SR Ca^{2+} leak, because of the exponential increase of leak-load relationship[49]; (2) expression and activity of NCX are increased in persAF, resulting in increased arrhythmogenic transient inward current in response to a given diastolic Ca^{2+} release from the SR[3]; (3) the distance between RyR clusters is reduced in AF, thereby enhancing the propagation of Ca^{2+} waves[50,51]; (4) impaired buffering of cytosolic Ca^{2+} promotes occurrence of atrial SCaEs in persAF, as demonstrated in this study.

Atrial Arrhythmias and Ca^{2+} Buffering

It has been established that alterations in cytosolic Ca^{2+} buffering contribute to ventricular arrhythmias.[13,23,52] To the best of our knowledge, there are currently no studies investigating the role of reduced Ca^{2+} buffering in atrial arrhythmogenesis in humans. It is often overlooked that only 1% of cytosolic Ca^{2+} is free and detected by conventional Ca^{2+} indicators such as Fluo-3, whereas the remainder is bound to Ca^{2+} buffers.[10] Because the myofilament protein cTnC is one of the major cytosolic Ca^{2+} buffers in cardiac myocytes,[10] it can be assumed that even minor changes in Ca^{2+} binding to cTnC can have major effects on free cytosolic Ca^{2+}, which could play an important role in cardiac arrhythmias. Early computational modeling studies, for example, suggested that Ca^{2+} buffers critically limit the diffusion of locally released Ca^{2+} and hamper activation of neighboring Ca^{2+} release sites, thereby preventing the occurrence of arrhythmogenic Ca^{2+} waves.[53] Accordingly, experimental reduction of cytosolic Ca^{2+} buffering caused increased Ca^{2+} sparks and intracellular propagation of arrhythmogenic Ca^{2+} waves.[54] Here we provide evidence that genetic downregulation of cTnC leads to significant reduction of cytosolic Ca^{2+} buffering and consecutively increased Ca^{2+} spark frequency. Furthermore, Ca^{2+} spark frequency could be reduced by pharmacological treatment with a Ca^{2+} sensitizing agent, EMD57033 (Figure 7). It is important to note that in si-cTnC iPSC-CMs, we found no difference, compared with control, in expression levels of RyR2, CaMKII, and junctophilin-2, nor the phosphorylated levels of RyR2 and CaMKII. Although RyR2 hyperphosphorylation is a well-accepted mechanism underlying increased diastolic Ca^{2+} leak in AF, the unaltered expression levels we found in our si-cTnC iPSC-CM model allowed us to focus on the contribution of reduced buffering to altered Ca^{2+} handling and arrhythmogenic activity.

Although several previous studies have investigated Ca^{2+} buffering properties in various animal models of AF, there have been contradictory results. Greiser et al found increased cytosolic Ca^{2+} buffering in a rabbit model after 5 days of atrial pacing.[11] They hypothesized that their observation of reduced cTnI phosphorylation, causing increased Ca^{2+}-cTnC binding, prevents detrimental effects of Ca^{2+} overload induced by rapid pacing. One could speculate that this may be an early response to high atrial stimulation frequencies, whereas loss of myofilament proteins, including cTnC, may represent a hallmark of late-stage remodeling, as shown by others.[14,50,55] Interestingly, mavacamten, a recently approved compound for hypertrophic cardiomyopathy treatment, reduces myofilament Ca^{2+} affinity and was found to increase incidence of AF in the PIONEER-HCM study (Phase 2 Open-label Pilot Study Evaluating Mavacamten in Subjects With Symptomatic Hypertrophic Cardiomyopathy and Left Ventricular Outflow Tract Obstruction),[56,57] suggesting that reduced Ca^{2+} buffering may indeed facilitate occurrence of atrial arrhythmias.

We observed AP alternans at low pacing frequencies in atrial iPSC-CMs with reduced Ca^{2+} buffering because of cTnC knockdown. Primary AP alternans is assumed to arise during pathological (steep) AP restitution, which was not observed here, pointing to underlying Ca^{2+}-driven alternans, which can canonically arise because of slow removal of Ca^{2+} into the SR, or in conditions of increased RyR2-mediated Ca^{2+} release into the cytosol. Because we detected significantly increased incidence of diastolic Ca^{2+} leak in atrial iPSC-CMs with reduced cTnC, we suggest that alternans arises at lower pacing rates, predominantly because of increased SCaEs, secondary to reduced buffer availability. This is in line with a previous modeling study suggesting that reduced cTnC-related Ca^{2+} buffering can increase Ca^{2+} alternans and also AP alternans.[58]

In addition to demonstrating the cellular arrhythmogenic phenotype caused by cTnC downregulation, we established the first ex vivo mouse heart model to investigate effects of reduced buffering on atrial arrhythmogenesis; we provided evidence at the whole-organ level that myofilament desensitization to Ca^{2+} increases susceptibility to atrial arrhythmia. Therefore, we hypothesize that reduced cytosolic Ca^{2+} buffering may play an important role in the progression and maintenance of AF in patients with persAF.

Potential Limitations

In our study, we collected samples from only 1 atrial region (right atrial appendage). Our findings may therefore not apply fully to other regions of the atria. Expression of α-actin and Tm2, for example, which was unaltered in our study of right atrial appendages, has been shown to be increased and decreased in left atrial biopsies from patients with AF, respectively.[44] The individuals from whom we obtained tissue samples included only patients who underwent coronary bypass or valve replacement surgery. Such individuals have numerous comorbidities, and the phenotype of atrial cardiac myocytes from our Ctrl patients may be different from nondiseased controls. Furthermore, it is unclear whether the mechanisms identified here also apply to patients with persAF without any heart disease. However, impaired contractile function is a common clinical finding throughout all atrial regions and in all patients with persAF.[2,40] Furthermore, ectopic activity occurs in right and left atria from patients with persAF, suggesting that increased incidence of SCaEs occurs throughout the whole atria. Here we demonstrate for the first time a direct mechanistic link between atrial hypocontractility and ectopic activity. Future clinical studies will be required to reveal whether there is a direct correlation between local hypocontractility and occurrence of ectopic activity in the different regions of the atria.

Our data suggest that loss of myofilament proteins and reduced expression of the major Ca^{2+} buffer cTnC are important contributors to reduced Ca^{2+} buffering in atrial cardiac myocytes from patients with persAF. There are numerous additional buffers that may contribute to impaired cytosolic Ca^{2+} buffering in AF, including the giant sarcomere protein titin,[59] as well as the important buffers SERCA and the sarcolemma.[10] However, activity of SERCA was comparable in persAF versus control cardiac myocytes investigated in our cohort (Figure 4), and cell capacitance as a marker for total membrane area was also comparable, making altered Ca^{2+} binding to SERCA and sarcolemma unlikely. Furthermore, the contribution of mitochondrial Ca^{2+} uptake to cytosolic Ca^{2+} buffering is controversial.[60–63] However, several studies have observed no impact of mitochondrial Ca^{2+} uptake on the amplitude of cytosolic Ca^{2+} transients, even during β-adrenergic stimulation where relevant Ca^{2+} accumulation into the mitochondrial matrix (to stimulate Krebs cycle dehydrogenases) occurs.[64–66] These observations render a significant contribution of mitochondria to cytosolic Ca^{2+} buffering unlikely. It needs to be considered that the concentration of cytosolic Ca^{2+} buffers is 3 times higher in the atria than in the ventricles.[10] This may also explain the relatively high buffer power observed in the present study.[10]

Because neither genetic mouse models of impaired myofilament Ca^{2+} binding nor specific pharmacological Ca^{2+} desensitizing agents are available, in the present study, we used the myosin ATPase inhibitor blebbistatin to indirectly modulate myofilament Ca^{2+} sensitivity in Langendorff-perfused mouse hearts. Blebbistatin is widely used as a contractile uncoupling agent for electrophysiological studies and has been shown to reduce Ca^{2+} sensitivity (pCa_{50}) of mouse skinned fiber preparations in a concentration-dependent manner.[52] Although minimal or nonsignificant effects on cardiac ion channels and APs by blebbistatin have been reported,[67] unspecific effects on ion channels cannot be completely excluded, in particular under the experimental conditions used in our model. However, atrial refractory periods, recorded at each experimental step (Figure S14B), did not differ between blebbistatin-treated and untreated hearts across the various K^+ concentrations. This suggests that increased susceptibility to atrial arrhythmia after blebbistatin treatment is indeed a result of impaired cytosolic Ca^{2+} buffering. Nevertheless, mouse models in general do not phenocopy all important aspects of human cardiac electrophysiology. Further extensive work in large-animal AF models will be required to investigate the time course and pathophysiological role of impaired Ca^{2+} buffering under conditions similar to those in patients who develop persAF.

Conclusions and Potential Significance

Here we provide evidence for a direct link between impaired atrial contractility in persAF and arrhythmogenesis. Our data show that loss of myofilament proteins, including reduced expression of cTnC, leads to reduced cytosolic Ca^{2+} buffering, which promotes the occurrence of SCaEs and increases susceptibility to atrial arrhythmia.

Because loss of myofilament proteins represents a rather late phenomenon in AF remodeling, this mechanism is likely to contribute to the chronification of the arrhythmia. Furthermore, because free cytosolic Ca^{2+} increase is believed to play a major role in electrical and structural remodeling,[45,68,69] reduced cytosolic Ca^{2+} buffering could therefore intensify remodeling in response to atrial tachycardia. In summary, our data suggest that, although the arrhythmogenic mechanisms of impaired Ca^{2+} buffering are not yet fully understood, the development of new strategies, specifically targeting intracellular Ca^{2+} buffering, may open novel therapeutic avenues to prevent progression and maintenance of AF. Already existing Ca^{2+} sensitizers, such as levosimendan and the indirectly acting omecamtiv mecarbil, may represent promising lead compounds.[70,71] Furthermore, nutrient supplements such as β-alanine and taurine, which have been demonstrated to increase intracellular Ca^{2+} buffering in cardiac myocytes, may be considered as valuable additions to currently available therapeutics used in AF management.[72,73]

ARTICLE INFORMATION

Received August 1, 2023; accepted May 31, 2024.

Affiliations

Cluster of Excellence "Multiscale Bioimaging: From Molecular Machines to Networks of Excitable Cells" (F.E.F., A.L., F.S., F.H., S.E.L., A.E., N.V.), Georg-August-University Göttingen, Germany. DZHK (German Centre for Cardiovascular Research), partner site Lower Saxony, Germany (F.E.F., D.H., V.M., I.S., A.L., Y.D., F.S., M. Gerloff, J.R.D.P., F.H., S.B., N.I., Y.B., S.K., A.E.-E., A.F.J., M. Großmann, B.C.D., H.B., I.K., W.A.L., S.E.L., G.K., A.E., F.E.M., N.V.). Institute of Pharmacology and Toxicology (F.E.F., D.H., V.M., I.S., A.L., Y.D., F.S., M. Gerloff, J.R.D.P., Y.B., S.K., F.E.M., N.V.), Department of Thoracic and Cardiovascular Surgery (F.H., A.E.-E., A.F.J., M. Großmann, B.C.D., H.B., I.K., G.K.), Department of Cardiology and Pneumology (S.B., N.I., W.A.L., S.E.L., A.E.), Heart Research Center Göttingen, University Medical Center Göttingen, Germany. Department of Thoracic and Cardiovascular Surgery (K.A., C.B.), Comprehensive Heart Failure Center Würzburg (K.A., C.B., C.M.), University Clinic Würzburg, Germany. Department of Thoracic and Cardiovascular Surgery, Klinikum Braunschweig, Germany (A.E.-E.). Department of Cardiology, University Hospital Heidelberg, Germany (C.S.). German Center for Cardiovascular Research Partner Site Heidelberg/Mannheim, Heidelberg University (C.S.). Department of Cardiology, University Hospital Giessen & Kerckhoff Clinic, Germany (S.S.). Department of Cardiology, Bad Nauheim & German Center for Cardiovascular Research Partner Site Rhine-Main, Germany (S.S.). Institute of Physiology II, University of Münster, Germany (W.A.L.). Gottfried Schatz Research Center, Division of Medical Physics and Biophysics, Medical University of Graz, Austria (J.H.). Department of Cardiology, Maastricht University Medical Centre and Cardiovascular Research Institute Maastricht, Maastricht University, The Netherlands (J.H.).

Acknowledgments

The authors are grateful to Lucie Carrier (Hamburg, Germany) for providing the antibody against phosphorylated cMyBP-C, and they would also like to thank David A. Eisner (Manchester, United Kingdom) for helpful discussion. Furthermore, the authors thank Ines Müller and Brigitte Korff for technical assistance and Maren Dilaj for secretarial help.

Sources of Funding

This work was supported by grants from the Deutsche Forschungsgemeinschaft to N.V. (DFG, VO 1568/3-1, VO1568/4-1) and to N.V. and S.E.L. (IRTG1816, SFB1002 and under Germany's Excellence Strategy-EXC 2067/1-390729940), from the Else-Kröner-Fresenius Foundation to N.V. (EKFS, 2016_A20), from the German Center for Cardiovascular Research to N.V. (DZHK, 81X4300102, 81X4300115, 81X4300112) and to A.E. (D81X4300123), and from the Bundesministerium für Bildung und Forschung (BMBF) subproject of the German Network for RASopathy Research (GeNeRARe) to G.K. (01GM1902D). This

ORIGINAL RESEARCH ARTICLE

work was further supported by scholarships from the Göttingen Promotionskolleg für Medizinstudierende, funded by the Jacob-Henle-Programm and the Else-Kröner-Fresenius-Stiftung to V.M. and from the German Academic Exchange Service to I.S. and N.I. We thank the Clinic for Cardiology and Pneumology at the University Medical Center Göttingen and the Deutsche Stiftung für Herzforschung (F/13/20) for funding provided to A.E.

Disclosures

None.

Supplemental Material

Supplemental Methods

Tables S1–S5

Figures S1–S14

Reference 74

REFERENCES

1. Go AS, Mozaffarian D, Roger VL, Benjamin EJ, Berry JD, Borden WB, Bravata DM, Dai S, Ford ES, Fox CS, et al; American Heart Association Statistics Committee and Stroke Statistics Subcommittee. Heart disease and stroke statistics--2013 update: a report from the American Heart Association. *Circulation*. 2013;127:e6–e245. doi: 10.1161/CIR.0b013e31828124ad
2. Goette A, Kalman JM, Aguinaga L, Akar J, Cabrera JA, Chen SA, Chugh SS, Corradi D, D'Avila A, Dobrev D, et al. EHRA/HRS/APHRS/SOLAECE expert consensus on atrial cardiomyopathies: definition, characterization, and clinical implication. *Heart Rhythm*. 2017;14:e3–e40. doi: 10.1016/j.hrthm.2016.05.028
3. Voigt N, Li N, Wang Q, Wang W, Trafford AW, Abu-Taha I, Sun Q, Wieland T, Ravens U, Nattel S, et al. Enhanced sarcoplasmic reticulum Ca^{2+} leak and increased Na^{+}-Ca^{2+} exchanger function underlie delayed afterdepolarizations in patients with chronic atrial fibrillation. *Circulation*. 2012;125:2059–2070. doi: 10.1161/CIRCULATIONAHA.111.067306
4. Voigt N, Heijman J, Wang Q, Chiang DY, Li N, Karck M, Wehrens XHT, Nattel S, Dobrev D. Cellular and molecular mechanisms of atrial arrhythmogenesis in patients with paroxysmal atrial fibrillation. *Circulation*. 2014;129:145–156. doi: 10.1161/CIRCULATIONAHA.113.006641
5. Dobrev D, Nattel S. Calcium handling abnormalities in atrial fibrillation as a target for innovative therapeutics. *J Cardiovasc Pharmacol*. 2008;52:293–299. doi: 10.1097/FJC.0b013e318171924d
6. Dobrev D, Voigt N, Wehrens XHT. The ryanodine receptor channel as a molecular motif in atrial fibrillation: pathophysiological and therapeutic implications. *Cardiovasc Res*. 2011;89:734–743. doi: 10.1093/cvr/cvq324
7. Neef S, Dybkova N, Sossalla S, Ort KR, Fluschnik N, Neumann K, Seipelt R, Schöndube FA, Hasenfuss G, Maier LS. CaMKII-dependent diastolic SR Ca^{2+} leak and elevated diastolic Ca^{2+} levels in right atrial myocardium of patients with atrial fibrillation. *Circ Res*. 2010;106:1134–1144. doi: 10.1161/CIRCRESAHA.109.203836
8. Hove-Madsen L, Llach A, Bayes-Genís A, Roura S, Font ER, Arís A, Cinca J. Atrial fibrillation is associated with increased spontaneous calcium release from the sarcoplasmic reticulum in human atrial myocytes. *Circulation*. 2004;110:1358–1363.
9. Bode D, Pronto JRD, Schiattarella GG, Voigt N. Metabolic remodelling in atrial fibrillation: manifestations, mechanisms and clinical implications [published online May 30, 2024]. *Nat Rev Cardiol*. doi: 10.1038/s41569-024-01038-6
10. Smith GL, Eisner DA. Calcium buffering in the heart in health and disease. *Circulation*. 2019;139:2358–2371. doi: 10.1161/CIRCULATIONAHA.118.039329
11. Greiser M, Kerfant B-G, Williams GSB, Voigt N, Harks E, Dibb KM, Giese A, Meszaros J, Verheule S, Ravens U, et al. Tachycardia-induced silencing of subcellular Ca^{2+} signaling in atrial myocytes. *J Clin Invest*. 2014;124:4759–4772. doi: 10.1172/JCI70102
12. Gomez-Hurtado N, Knollmann BC. Calcium in atrial fibrillation - pulling the trigger or not? *J Clin Invest*. 2014;124:4684–4686. doi: 10.1172/JCI77986
13. Eisner D, Neher E, Taschenberger H, Smith G. Physiology of intracellular calcium buffering. *Physiol Rev*. 2023;103:2767–2845. doi: 10.1152/physrev.00042.2022
14. Ke L, Qi XY, Dijkhuis A-J, Chartier D, Nattel S, Henning RH, Kampinga HH, Brundel BJJM. Calpain mediates cardiac troponin degradation and contractile dysfunction in atrial fibrillation. *J Mol Cell Cardiol*. 2008;45:685–693. doi: 10.1016/j.yjmcc.2008.08.012
15. Allessie M, Ausma J, Schotten U. Electrical, contractile and structural remodeling during atrial fibrillation. *Cardiovasc Res*. 2002;54:230–246. doi: 10.1016/s0008-6363(02)00258-4
16. Eiras S, Narolska NA, van Loon RB, Boontje NM, Zaremba R, Jimenez CR, Visser FC, Stooker W, van der Velden J, Stienen GJM. Alterations in contractile protein composition and function in human atrial dilatation and atrial fibrillation. *J Mol Cell Cardiol*. 2006;41:467–477. doi: 10.1016/j.yjmcc.2006.06.072
17. Belus A, Piroddi N, Ferrantini C, Tesi C, Cazorla O, Toniolo L, Drost M, Mearini G, Carrier L, Rossi A, et al. Effects of chronic atrial fibrillation on active and passive force generation in human atrial myofibrils. *Circ Res*. 2010;107:144–152. doi: 10.1161/CIRCRESAHA.110.220699
18. Voigt N, Zhou XB, Dobrev D. Isolation of human atrial myocytes for simultaneous measurements of Ca^{2+} transients and membrane currents. *J Vis Exp*. 2013;77:e50235. doi: 10.3791/50235
19. Cyganek L, Tiburcy M, Sekeres K, Gerstenberg K, Bohnenberger H, Lenz C, Henze S, Stauske M, Salinas G, Zimmermann W-H, et al. Deep phenotyping of human induced pluripotent stem cell-derived atrial and ventricular cardiomyocytes. *JCI Insight*. 2018;3:e99941. doi: 10.1172/jci.insight.99941
20. Seibertz F, Rubio T, Springer R, Popp F, Ritter M, Liutkute A, Bartelt L, Stelzer L, Haghighi F, Pietras J, et al. Atrial fibrillation-associated electrical remodelling in human induced pluripotent stem cell-derived atrial cardiomyocytes: a novel pathway for antiarrhythmic therapy development. *Cardiovasc Res*. 2023;119:2623–2637. doi: 10.1093/cvr/cvad143
21. Rössler U, Hennig AF, Stelzer N, Bose S, Kopp J, Søe K, Cyganek L, Zifarelli G, Ali S, von der Hagen M, et al. Efficient generation of osteoclasts from human induced pluripotent stem cells and functional investigations of lethal CLCN7-related osteopetrosis. *J Bone Miner Res*. 2021;36:1621–1635. doi: 10.1002/jbmr.4322
22. Hwang HS, Kryshtal DO, Feaster TK, Sánchez-Freire V, Zhang J, Kamp TJ, Hong CC, Wu JC, Knollmann BC. Comparable calcium handling of human iPSC-derived cardiomyocytes generated by multiple laboratories. *J Mol Cell Cardiol*. 2015;85:79–88. doi: 10.1016/j.yjmcc.2015.05.003
23. Jung P, Seibertz F, Fakuade FE, Ignatyeva N, Sampathkumar S, Ritter M, Li H, Mason FE, Ebert A, Voigt N. Increased cytosolic calcium buffering contributes to a cellular arrhythmogenic substrate in iPSC-cardiomyocytes from patients with dilated cardiomyopathy. *Basic Res Cardiol*. 2022;117:5. doi: 10.1007/s00395-022-00912-z
24. Seibertz F, Reynolds M, Voigt N. Single-cell optical action potential measurement in human induced pluripotent stem cell-derived cardiomyocytes. *J Vis Exp*. 2020;166:e61890. doi: 10.3791/61890
25. Walden AP, Dibb KM, Trafford AW. Differences in intracellular calcium homeostasis between atrial and ventricular myocytes. *J Mol Cell Cardiol*. 2009;46:463–473. doi: 10.1016/j.yjmcc.2008.11.003
26. Morano I, Hofmann F, Zimmer M, Rüegg JC. The influence of P-light chain phosphorylation by myosin light chain kinase on the calcium sensitivity of chemically skinned heart fibres. *FEBS Lett*. 1985;189:221–224. doi: 10.1016/0014-5793(85)81027-9
27. Fabiato A, Fabiato F. Excitation-contraction coupling of isolated cardiac fibers with disrupted or closed sarcolemmas. Calcium-dependent cyclic and tonic contractions. *Circ Res*. 1972;31:293–307. doi: 10.1161/01.res.31.3.293
28. Arteaga GM, Warren CM, Milutinovic S, Martin AF, Solaro RJ. Specific enhancement of sarcomeric response to Ca^{2+} protects murine myocardium against ischemia-reperfusion dysfunction. *Am J Physiol Heart Circ Physiol*. 2005;289:H2183–H2192. doi: 10.1152/ajpheart.00520.2005
29. Seibertz F, Sutanto H, Dülk R, Pronto JRD, Springer R, Rapedius M, Liutkute A, Ritter M, Jung P, Stelzer L, et al. Electrophysiological and calcium-handling development during long-term culture of human-induced pluripotent stem cell-derived cardiomyocytes. *Basic Res Cardiol*. 2023;118:14. doi: 10.1007/s00395-022-00973-0
30. Bruegmann T, Beiert T, Vogt CC, Schrickel JW, Sasse P. Optogenetic termination of atrial fibrillation in mice. *Cardiovasc Res*. 2018;114:713–723. doi: 10.1093/cvr/cvx250
31. Trafford AW, Díaz ME, Eisner DA. A novel, rapid and reversible method to measure Ca^{2+} buffering and time-course of total sarcoplasmic reticulum Ca^{2+} content in cardiac ventricular myocytes. *Pflugers Arch*. 1999;437:501–503. doi: 10.1007/s004240050808
32. Díaz ME, Trafford AW, Eisner DA. The effects of exogenous calcium buffers on the systolic calcium transient in rat ventricular myocytes. *Biophys J*. 2001;80:1915–1925. doi: 10.1016/S0006-3495(01)76161-9
33. Shannon TR, Ginsburg KS, Bers DM. Quantitative assessment of the SR Ca^{2+} leak-load relationship. *Circ Res*. 2002;91:594–600. doi: 10.1161/01.res.0000036914.12686.28
34. Heijman J, Muna AP, Veleva T, Molina CE, Sutanto H, Tekook M, Wang Q, Abu-Taha IH, Gorka M, Künzel S, et al. Atrial myocyte NLRP3/CaMKII nexus forms a substrate for postoperative atrial fibrillation. *Circ Res*. 2020;127:1036–1055. doi: 10.1161/CIRCRESAHA.120.316710
35. Grandi E, Pandit SV, Voigt N, Workman AJ, Dobrev D, Jalife J, Bers DM. Human atrial action potential and Ca^{2+} model: sinus rhythm

and chronic atrial fibrillation. *Circ Res*. 2011;109:1055–1066. doi: 10.1161/CIRCRESAHA.111.253955
36. Wang Z, Nattel S, Yue L, Gaspo R, Feng J, Li G-R. Ionic remodeling underlying action potential changes in a canine model of atrial fibrillation. *Circ Res*. 2012;81:512–525.
37. Van Wagoner DR, Pond AL, Lamorgese M, Rossie SS, McCarthy PM, Nerbonne JM. Atrial L-type Ca^{2+} currents and human atrial fibrillation. *Circ Res*. 1999;85:428–436. doi: 10.1161/01.res.85.5.428
38. Christ T, Boknik P, Wöhrl S, Wettwer E, Graf EM, Bosch RF, Knaut M, Schmitz W, Ravens U, Dobrev D. L-type Ca^{2+} current downregulation in chronic human atrial fibrillation is associated with increased activity of protein phosphatases. *Circulation*. 2004;110:2651–2657. doi: 10.1161/01.CIR.0000145659.80212.6A
39. Aimé-Sempé C, Folliguet T, Rücker-Martin C, Krajewska M, Krajewska S, Heimburger M, Aubier M, Mercadier JJ, Reed JC, Hatem SN. Myocardial cell death in fibrillating and dilated human right atria. *J Am Coll Cardiol*. 1999;34:1577–1586. doi: 10.1016/s0735-1097(99)00382-4
40. Schotten U, Ausma J, Stellbrink C, Sabatschus I, Vogel M, Frechen D, Schoendube F, Hanrath P, Allessie MA. Cellular mechanisms of depressed atrial contractility in patients with chronic atrial fibrillation. *Circulation*. 2001;103:691–698. doi: 10.1161/01.cir.103.5.691
41. Logan WF, Rowlands DJ, Howitt G, Holmes AM. Left atrial activity following cardioversion. *Lancet*. 1965;2:471–473. doi: 10.1016/s0140-6736(65)91427-3
42. Lenaerts I, Bito V, Heinzel FR, Driesen RB, Holemans P, D'hooge J, Heidbüchel H, Sipido KR, Willems R. Ultrastructural and functional remodeling of the coupling between Ca^{2+} influx and sarcoplasmic reticulum Ca^{2+} release in right atrial myocytes from experimental persistent atrial fibrillation. *Circ Res*. 2009;105:876–885. doi: 10.1161/CIRCRESAHA.109.206276
43. Li N, Brundel BJJM. Inflammasomes and proteostasis novel molecular mechanisms associated with atrial fibrillation. *Circ Res*. 2020;127:73–90. doi: 10.1161/CIRCRESAHA.119.316364
44. Rennison JH, Li L, Lin CR, Lovano BS, Castel L, Wass SY, Cantlay CC, McHale M, Gillinov AM, Mehra R, et al. Atrial fibrillation rhythm is associated with marked changes in metabolic and myofibrillar protein expression in left atrial appendage. *Pflugers Arch*. 2021;473:461–475. doi: 10.1007/s00424-021-02514-5
45. Makary S, Voigt N, Maguy A, Wakili R, Nishida K, Harada M, Dobrev D, Nattel S. Differential protein kinase C isoform regulation and increased constitutive activity of acetylcholine-regulated potassium channels in atrial remodeling. *Circ Res*. 2011;109:1031–1043. doi: 10.1161/CIRCRESAHA.111.253120
46. Morano I. Tuning the human heart molecular motors by myosin light chains. *J Mol Med (Berl)*. 1999;77:544–555. doi: 10.1007/s001099900031
47. Kockskämper J, Khafaga M, Grimm M, Elgner A, Walther S, Kockskämper A, von Lewinski D, Post H, Grossmann M, Dörge H, et al. Angiotensin II and myosin light-chain phosphorylation contribute to the stretch-induced slow force response in human atrial myocardium. *Cardiovasc Res*. 2008;79:642–651. doi: 10.1093/cvr/cvn126
48. El-Armouche A, Boknik P, Eschenhagen T, Carrier L, Knaut M, Ravens U, Dobrev D. Molecular determinants of altered Ca^{2+} handling in human chronic atrial fibrillation. *Circulation*. 2006;114:670–680. doi: 10.1161/CIRCULATIONAHA.106.636845
49. Bers DM. Cardiac sarcoplasmic reticulum calcium leak: basis and roles in cardiac dysfunction. *Annu Rev Physiol*. 2014;76:107–127. doi: 10.1146/annurev-physiol-020911-153308
50. Macquaide N, Tuan H-TM, Hotta J-I, Sempels W, Lenaerts I, Holemans P, Hofkens J, Jafri MS, Willems R, Sipido KR. Ryanodine receptor cluster fragmentation and redistribution in persistent atrial fibrillation enhance calcium release. *Cardiovasc Res*. 2015;108:387–398. doi: 10.1093/cvr/cvv231
51. Sutanto H, van Sloun B, Schönleitner P, van Zandvoort MAMJ, Antoons G, Heijman J. The subcellular distribution of ryanodine receptors and L-type Ca^{2+} channels modulates Ca^{2+}-transient properties and spontaneous Ca^{2+}-release events in atrial cardiomyocytes. *Front Physiol*. 2018;9:1108. doi: 10.3389/fphys.2018.01108
52. Baudenbacher F, Schober T, Pinto JR, Sidorov VY, Hilliard F, Solaro RJ, Potter JD, Knollmann BC. Myofilament Ca^{2+} sensitization causes susceptibility to cardiac arrhythmia in mice. *J Clin Invest*. 2008;118:3893–3903. doi: 10.1172/JCI36642
53. Keizer J, Smith GD, Ponce-Dawson S, Pearson JE. Saltatory propagation of Ca^{2+} waves by Ca^{2+} sparks. *Biophys J*. 1998;75:595–600. doi: 10.1016/S0006-3495(98)77550-2
54. Bovo E, Mazurek SR, Fill M, Zima AV. Cytosolic Ca^{2+} buffering determines the intra-SR Ca^{2+} concentration at which cardiac Ca^{2+} sparks terminate. *Cell Calcium*. 2015;58:246–253. doi: 10.1016/j.ceca.2015.06.002
55. Ausma J, Litjens N, Lenders MH, Duimel H, Mast F, Wouters L, Ramaekers F, Allessie M, Borgers M. Time course of atrial fibrillation-induced cellular structural remodeling in atria of the goat. *J Mol Cell Cardiol*. 2001;33:2083–2094. doi: 10.1006/jmcc.2001.1472
56. Heitner SB, Jacoby D, Lester SJ, Owens A, Wang A, Zhang D, Lambing J, Lee J, Semigran M, Sehnert AJ. Mavacamten treatment for obstructive hypertrophic cardiomyopathy: a clinical trial. *Ann Intern Med*. 2019;170:741–748. doi: 10.7326/M18-3016
57. Masri A, Olivotto I. Cardiac myosin inhibitors as a novel treatment option for obstructive hypertrophic cardiomyopathy: addressing the core of the matter. *J Am Heart Assoc*. 2022;11:e024656. doi: 10.1161/JAHA.121.024656
58. Zile MA, Trayanova NA. Increased thin filament activation enhances alternans in human chronic atrial fibrillation. *Am J Physiol Heart Circ Physiol*. 2018;315:H1453–H1462. doi: 10.1152/ajpheart.00658.2017
59. Labeit D, Watanabe K, Witt C, Fujita H, Wu Y, Lahmers S, Funck T, Labeit S, Granzier H. Calcium-dependent molecular spring elements in the giant protein titin. *Proc Natl Acad Sci USA*. 2003;100:13716–13721. doi: 10.1073/pnas.2235652100
60. Mason FE, Pronto JRD, Alhussini K, Maack C, Voigt N. Cellular and mitochondrial mechanisms of atrial fibrillation. *Basic Res Cardiol*. 2020;115:72. doi: 10.1007/s00395-020-00827-7
61. Williams GSB, Boyman L, Chikando AC, Khairallah RJ, Lederer WJ. Mitochondrial calcium uptake. *Proc Natl Acad Sci USA*. 2013;110:10479–10486. doi: 10.1073/pnas.1300410110
62. Hamilton S, Terentyeva R, Clements RT, Belevych AE, Terentyev D. Sarcoplasmic reticulum-mitochondria communication; implications for cardiac arrhythmia. *J Mol Cell Cardiol*. 2021;156:105–113. doi: 10.1016/j.yjmcc.2021.04.002
63. Mackenzie L, Roderick HL, Berridge MJ, Conway SJ, Bootman MD. The spatial pattern of atrial cardiomyocyte calcium signalling modulates contraction. *J Cell Sci*. 2004;117:6327–6337. doi: 10.1242/jcs.01559
64. Lu X, Ginsburg KS, Kettlewell S, Bossuyt J, Smith GL, Bers DM. Measuring local gradients of intramitochondrial [Ca^{2+}] in cardiac myocytes during sarcoplasmic reticulum Ca^{2+} release. *Circ Res*. 2013;112:424–431. doi: 10.1161/CIRCRESAHA.111.300501
65. Kohlhaas M, Liu T, Knopp A, Zeller T, Ong MF, Böhm M, O'Rourke B, Maack C. Elevated cytosolic Na^{+} increases mitochondrial formation of reactive oxygen species in failing cardiac myocytes. *Circulation*. 2010;121:1606–1613. doi: 10.1161/CIRCULATIONAHA.109.914911
66. Kwong JQ, Lu X, Correll RN, Schwanekamp JA, Vagnozzi RJ, Sargent MA, York AJ, Zhang J, Bers DM, Molkentin JD. The mitochondrial calcium uniporter selectively matches metabolic output to acute contractile stress in the heart. *Cell Rep*. 2015;12:15–22. doi: 10.1016/j.celrep.2015.06.002
67. Fedorov VV, Lozinsky IT, Sosunov EA, Anyukhovsky EP, Rosen MR, Balke CW, Efimov IR. Application of blebbistatin as an excitation-contraction uncoupler for electrophysiologic study of rat and rabbit hearts. *Heart Rhythm*. 2007;4:619–626. doi: 10.1016/j.hrthm.2006.12.047
68. Li N, Chiang DY, Wang S, Wang Q, Sun L, Voigt N, Respress JL, Ather S, Skapura DG, Jordan VK, et al. Ryanodine receptor-mediated calcium leak drives progressive development of an atrial fibrillation substrate in a transgenic mouse model. *Circulation*. 2014;129:1276–1285. doi: 10.1161/CIRCULATIONAHA.113.006611
69. Qi XY, Yeh Y-H, Xiao L, Burstein B, Maguy A, Chartier D, Villeneuve LR, Brundel BJJM, Dobrev D, Nattel S. Cellular signaling underlying atrial tachycardia remodeling of L-type calcium current. *Circ Res*. 2008;103:845–854. doi: 10.1161/CIRCRESAHA.108.175463
70. Abacilar AF, Dogan OF. Levosimendan use decreases atrial fibrillation in patients after coronary artery bypass grafting: a pilot study. *Heart Surg Forum*. 2013;16:E287–E294. doi: 10.1532/hsf98.2013190
71. Malik FI, Hartman JJ, Elias KA, Morgan BP, Rodriguez H, Brejc K, Anderson RL, Sueoka SH, Lee KH, Finer JT, et al. Cardiac myosin activation: a potential therapeutic approach for systolic heart failure. *Science*. 2011;331:1439–1443. doi: 10.1126/science.1200113
72. Eley DW, Lake N, Ter Keurs HEDJ. Taurine depletion and excitation-contraction coupling in rat myocardium. *Circ Res*. 1994;74:1210–1219.
73. Creighton JV, de Souza Gonçalves L, Artioli GG, Tan D, Elliott-Sale KJ, Turner MD, Doig CL, Sale C. Physiological roles of carnosine in myocardial function and health. *Adv Nutr*. 2022;13:1914–1929. doi: 10.1093/advances/nmac059
74. Seibertz F, Rapedius M, Fakuade FE, Tomsits P, Liutkute A, Cyganek L, Becker N, Majumder R, Clauß S, Fertig N, et al. A modern automated patch-clamp approach for high throughput electrophysiology recordings in native cardiomyocytes. *Commun Biol*. 2022;5:969. doi: 10.1038/s42003-022-03871-2

ORIGINAL RESEARCH ARTICLE